AFSWC-TR-65-6

AFSWC-TR
65-6

PAYLOAD FOR ALARR

Alan Haire

Aerolab Development Company
Monrovia, California

Contract AF 29(601)-6248

TECHNICAL REPORT NO. AFSWC-TR-65-6

March 1966

AIR FORCE SPECIAL WEAPONS CENTER
Air Force Systems Command
Kirtland Air Force Base
New Mexico

AFSWC-TR-65-6

AIR FORCE SPECIAL WEAPONS CENTER
Air Force Systems Command
Kirtland Air Force Base
New Mexico

AFSWC-TR-65-6

PAYLOAD FOR ALARR

Alan Haire

Aerolab Development Company
Monrovia, California
Contract AF 29(601)-6248

TECHNICAL REPORT NO. AFSWC-TR-65-6

FOREWORD

This report was prepared by the Aerolab Development Company, Monrovia, California, under Contract AF 29(601)-6248. The research was performed under Program Element 6.54.02.21.4, ESP 921A-9087-02119-2119T462.

Inclusive dates of research were October 1963 through November 1965. The report was submitted 13 February 1966 by the Air Force Special Weapons Center Test Director, 1Lt Richard G. Grisham (SWTSS).

This report has been reviewed and is approved.

Richard G. Grisham

RICHARD G. GRISHAM
1Lt, USAF
Test Director

Noel D. Austin

NOEL D. AUSTIN
Colonel, USAF
Assistant Deputy for Test
and Engineering

Lewis M. Hatch

LEWIS M. HATCH
Colonel, USAF
Plans & Requirements Office

ABSTRACT

A development program was undertaken to provide an air sampling payload for the Air-Launched, Air-Recoverable Rocket (ALARR) vehicle. The purpose of the payload was to collect samples of particulate radioactive debris from the atmosphere. The payload was to be capable of operating in narrow altitude bands between 70,000 and 150,000 feet, be capable of filtering the largest volume of air possible through IPC 1478 filter paper, and be compatible with the ALARR vehicle. Development included design, fabrication, ground testing (including environmental, functional, and flow calibration testing), and flight testing. This report contains the description of the payload, the design analysis, and the results of the ground testing.

CONTENTS

ILLUSTRATIONS

TABLES

SECTION I

INTRODUCTION

This report describes the analysis, design, and testing performed by Aerolab Development Company in the development of a payload for ALARR under Contract No. AF 29(601)-6248 for the Air Force Special Weapons Center (AFSWC). The development began 28 October 1963.

Requirements of the payload were

a. Compatibility with the ALARR vehicle.

b. Weight of 135 $\pm$ 5 pounds, with the center of gravity forward of missile station 18.0 (for aerodynamic stability of the ALARR vehicle).

c. Filtration of large volumes of air while moving in a relatively flat trajectory through any altitude between 70,000 and 150,000 feet.

d. Filtration of the maximum possible volume flow of air, consistent with other requirements.

e. Ease of disassembly and assembly, particularly of the filter paper.

f. A smooth and highly polished internal finish to allow for thorough decontamination.

g. Reusability with a minimum amount of time and effort.

h. Filter paper to be IPC 1478 and of maximum size, consistent with proper aerodynamics and good design practices.

i. Capability to commence and terminate sampling upon receipt of a signal from a pre-set timer in the recovery section of the ALARR vehicle.

j. Ability to sample at a maximum Mach number of 3.2 at any altitude between 70,000 and 150,000 feet.

One payload was to be structurally tested to 150 percent of maximum design conditions, including acceleration, shock, and vibration. One payload was to be functionally tested to ensure proper electrical and mechanical operation. One payload was to be flow tested in a wind tunnel to determine flow rate through the filter for various altitudes and Mach numbers.

SECTION II

CONFIGURATION

The general configuration of the payload is shown in Figure 1. Details are shown in the drawings in the 63J15400 Data List, Payload ALARR. Major items are:

a. Nose Tip Assembly

The nose tip assembly consists basically of a split fiberglass tip held together with an explosive actuator. When ignited, the actuator pushes the two halves of the tip apart and away from the payload. The combustion gases are retained in the actuator.

b. Outer Shell

The outer shell is basically an ogive fiberglass shell with an ablative coating for thermal protection.

c. Inlet Assembly

The major components of the inlet assembly are the inlet, splitter plate, door, and door actuating and positioning mechanism. The inside of the inlet is a straight cylinder. The splitter plate divides the inlet into two halves at the forward end. The door is an extension of the splitter plate when in the open position. It closes by rotating 90° and sealing against the inlet by means of an O-ring. A precoiled torsion spring provides the force to close the door. The door is held open by an explosive bolt, which is ignited to allow the door to close. An adjustable bolt stops the door in the closed position.

d. Basket Assembly

The basket assembly includes the filter paper basket contained between two screen baskets.

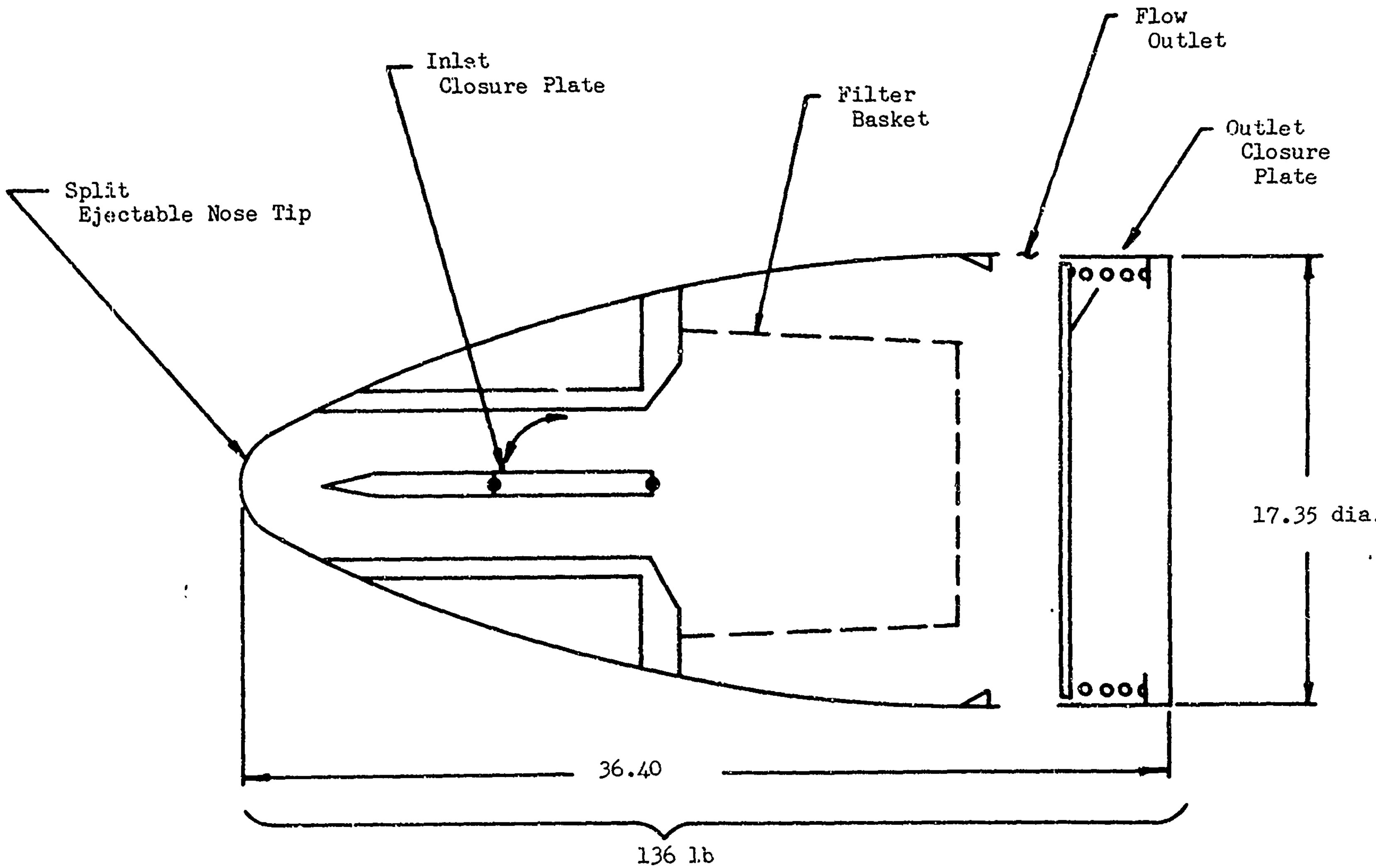

Figure 1. PAYLOAD CONFIGURATION

e. Band Assembly

The band assembly is basically a flat spring metal band which is wrapped around the air outlet at the aft end of the outer shell. It is held in place by an explosive bolt that releases the band when ignited. A piece of thin foil prevents the gases from the bolt from entering the payload.

f. Aft Assembly

The aft assembly includes the ring for mounting on the ALARR vehicle, the explosive squibs power supply (including batteries, heater, and thermostat), and the sealing plate and its actuating mechanism. The sealing plate closes off the air outlet by moving forward and sealing against a gasket on the outer shell. A precompressed compression spring provides the force to move and seal the plate. The plate is held back by an explosive bolt which is ignited to allow the plate to close.

SECTION III

FLOW ANALYSIS

1. Air Flow

Flow around and through the payload was analyzed by the following methods:

a. Inlet

Flow into the inlet consists of a series of oblique shocks off the splitter plate, inlet, and door. Rigorous analysis is not possible, but it is known that the pressure recovery is greater than for a normal shock. The pressure recovery was conservatively assumed to be that across a normal shock. Flow on the exterior of the inlet would be an oblique shock off the inlet lip.

b. Outer Shell

Flow around the outer shell was analyzed as a two-dimensional Prandtl-Meyer expansion to the flow outlet at the aft end. The actual expansion is three dimensional; therefore, the aft pressure would be lower than that conservatively calculated.

c. Outlet

Flow at the outlet was analyzed by an approximate method developed for analysis of secondary injection for thrust vector control. Experiments showed that the approximation gave higher injection pressures than actual; therefore, the analysis is again conservative.

d. Filter

Flow through the filter was determined from the calibration curve developed by the Institute of Paper Chemistry. Figure 2 and

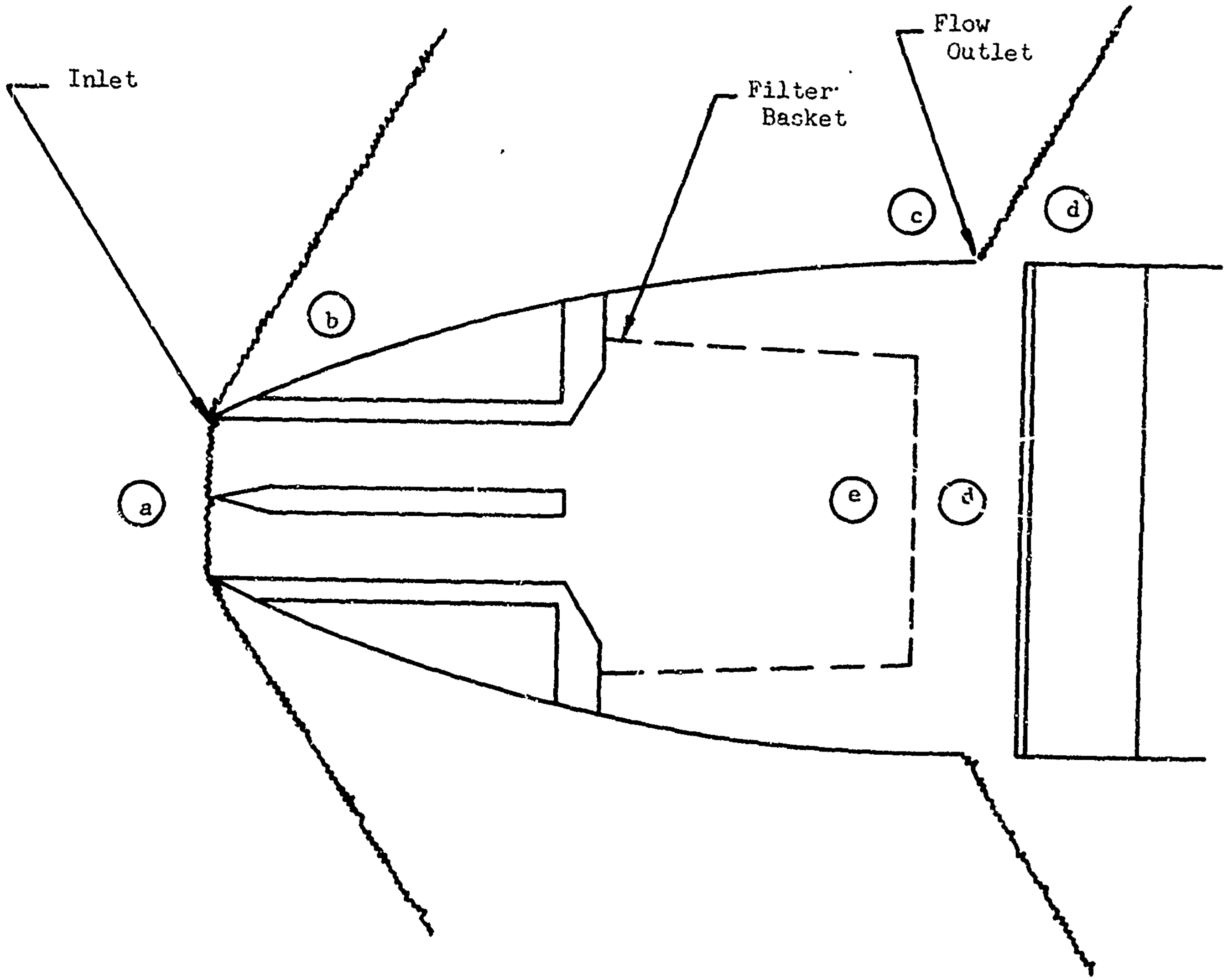

Figure 2. FLOW ANALYSIS MODEL

table 1 show the details of the calculation method. The calculations were performed on a computer, and the results were (1) weight flow rate intercepted by the inlet, (2) maximum weight flow rate that can be passed through the filter basket (assuming attached shock at inlet), and (3) ratio of filter to intercepted weight flow rates (or flow intake efficiency). These were determined as functions of altitude and Mach number. The results are plotted in figures 3, 4, and 5. Thus, for any given trajectory the weight flow rate can be integrated along the trajectory to find the total weight of air sampled. By using the flow intake efficiency curve, the total volume flow can be similarly found.

The filter flow rate is a maximum; therefore, when it is greater than the inlet flow rate, the actual flow rate is that intercepted by the inlet. When the filter flow rate is less than the inlet flow rate, spillage will occur and the shock will become detached. Rigorous flow analysis is virtually impossible under this condition; therefore, the analysis for the attached shock is used for this condition also. The flow rate ratio then represents the fraction of the intercepted air that is "swallowed," and the remainder represents that which is "spilled."

The entire analysis is not completely rigorous, but is all that is possible and/or justified for such a complex configuration. Final flow characteristics must be determined by tests of the payload.

2. Inlet

Inlet diameter = 5.973 inches (Ref: Dwg 53J15422)

$$\text{Inlet area} = \frac{\pi}{4}\left(\frac{5.973}{12}\right)^2$$

$$= 0.1946 \text{ ft}^2$$

$$= A_1$$

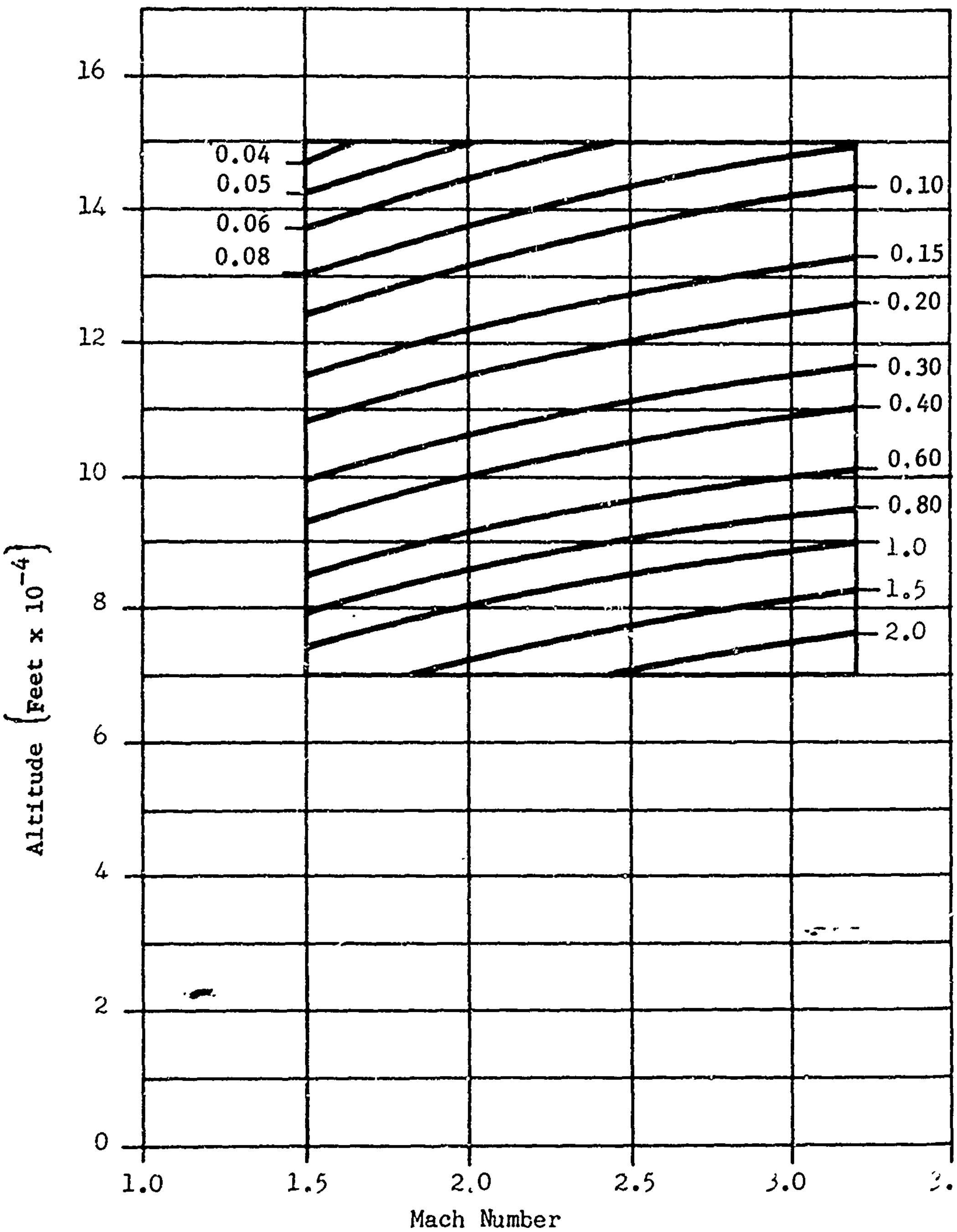

Figure 3. MASS FLOW RATE INTERCEPTED BY INLET (lb/sec)

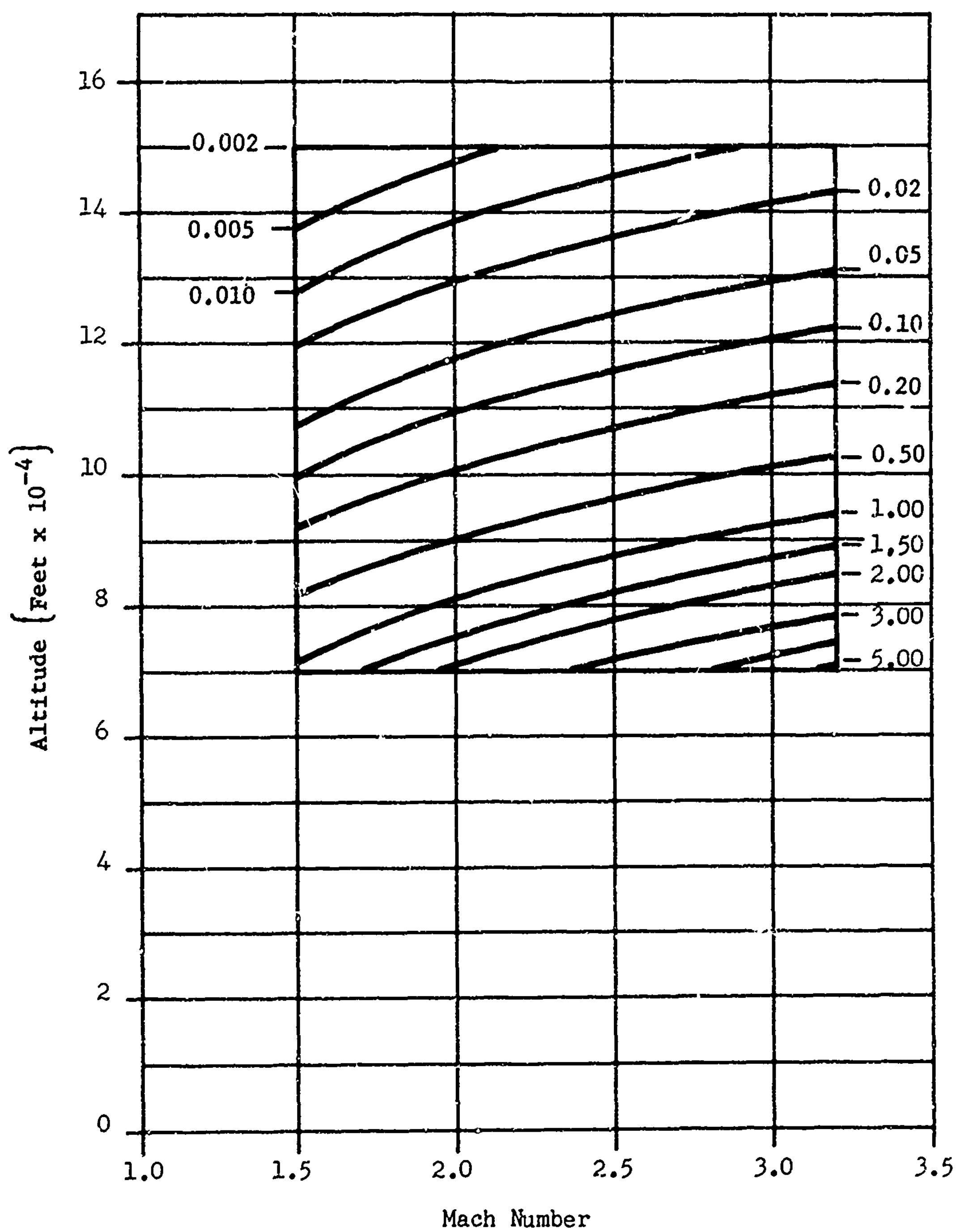

Figure 4. MAXIMUM WEIGHT FLOW RATE THRU BASKET (lb/sec)

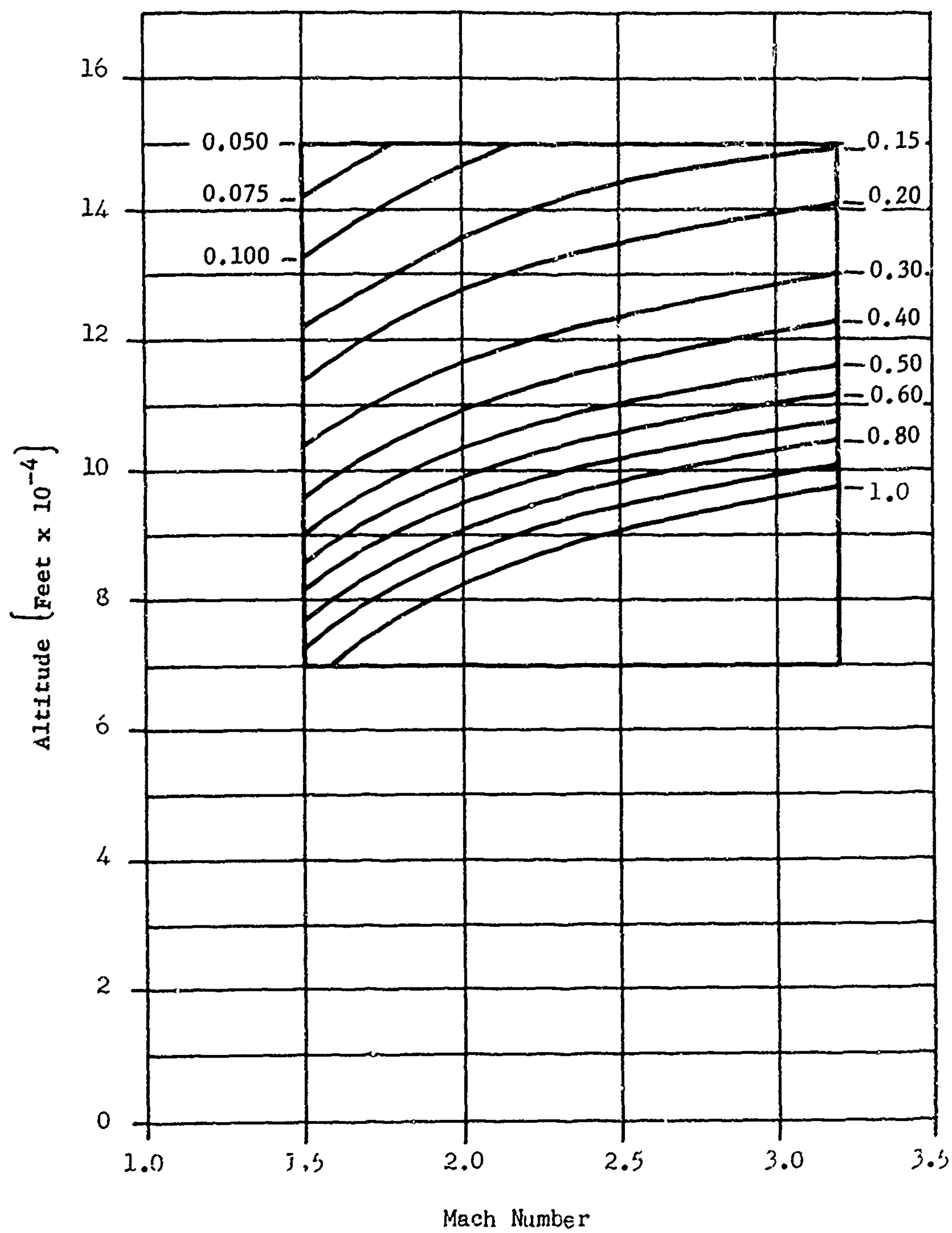

Figure 5. FLOW INTAKE EFFICIENCY

3. Basket

Figure 6 shows the geometry and dimensions of the basket.

Screen: **Wire diameter 0.017, 0.125 spacing both ways.**

Expanded metal: 3/4" - No. 16 flattened.

Rods: 1.87 diameter, 1.00 spacing one way.

(Reference Dwg 63D15440 and subassemblies)

a. Basket Area

$$\frac{\pi}{4}(11.62)^2 + \pi\left(\frac{12.53 + 11.62}{2}\right)9.15 = 106.0$$

$$+ 347.0 = 453.0 \text{ in}^2$$

$$\text{Screen open area} = \left(\frac{0.125 - 0.017}{0.125}\right)^2 = 0.746$$

Expanded metal open area (3/4" - No. 16 flattened) = 0.73 (Reference 30)

$$\text{Rods open area} = \frac{1.000 - 0.187}{1.000} = 0.813$$

$$\text{Cylinder area} = (347.0)(0.746)(0.73) = 189.0$$

$$\text{Bottom area} = (106.0)(0.746)(0.73)(0.813) = 47.0$$

$$\text{Total} = 236.0 \text{ in}^2$$

$$= 1.640 \text{ ft}^2$$

$$= A_2$$

$$\text{Average open area} = \frac{236.0}{453.0} = 0.521$$

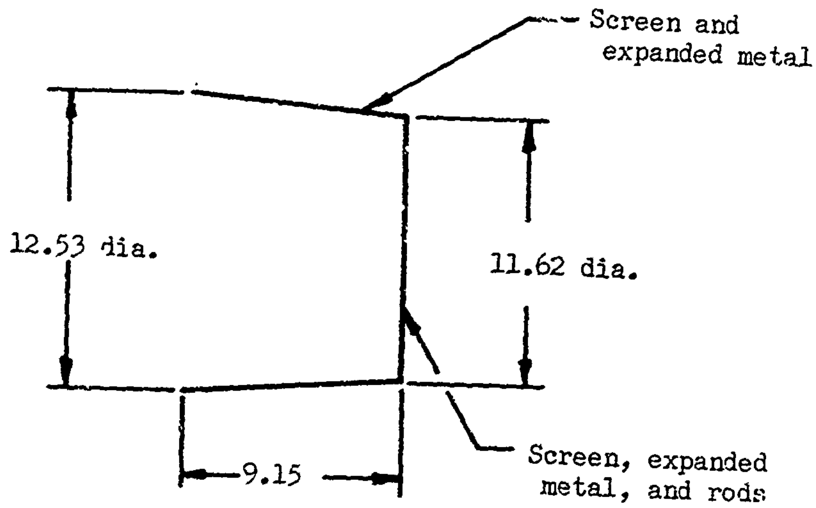

Figure 6. BASKET GEOMETRY & DIMENSIONS

TABLE I

FLOW CALCULATION METHOD

VARIABLE	SOURCE	
M_1	Given	
M_2	M_1, $\theta_1 (19^\circ 30')$	(Ref 26, page 7-32, 7-33)
ν_2	M_1 -	(Ref 5, table II)
ν_3	$\nu_2 + \left(\theta_2 - \theta_1\right) = \nu_2 + 0.32409$	
M_3	ν_3	(Ref 5, table II)

In all cases between 70,000 ft and 150,000 ft and Mach 1.5 to 3.2, $M_3 \geq M_1$. This is not physically possible; therefore, it is due to mixing two and three dimensional analysis. Maximum possible value of M_3 is M_1; therefore, assume $M_3 = M_1$ in all cases. Accordingly, $P_3 = P_1$.

h_1	Given	
$P_1 \left(= P_3\right)$	h_1	(Ref 6, table IIA)
P_4/P_3	$M_3 \left(=M_1\right)$	(Ref 27, figure 17)
P_4	$\left(P_r/P_3\right)\left(P_1\right)$	
P_1/P_5	M_1	$\left(\text{Ref 5, table II, } P_1/P_{t_2}\right)$ (Assume full stagnation because of 8.4:1 area ratio)
P_5	$P_1/\left(P_1/P_5\right)$	
T_1	h_1	(Ref 6, table IIA)
T_1/T_5	M_1	$\left(\text{Ref 5, table II, } T/T_t\right)$ (Assume full stagnation because of 8.4:1 area ratio)

TABLE I (Cont'd)

FLOW CALCULATION METHOD

VARIABLE	SOURCE	
T_5	$T_1\{T_1/T_5\}$	
ρ_5	P_5/RT_5 (R = 53.3 ft lb /lb^{o}R) Perfect Gas Law	
ρ_4	P_4/RT_5 (R = 53.3 ft lb /lb^{o}R) Perfect Gas Law $\{T_5$ used per reference 27, page 44$\}$	
$\bar{\sigma}$	$\{\rho_4 + \rho_5\}/(2)(0.0765)$	(Ref 28, page 44)
ΔP	$P_5 - P_4$	
μ	T_5	(Ref 29, page 1-69, 1-70)
	$/0.3737 \times 10^{-6}$	(Ref 28, page 44)
$\bar{\sigma}\,\bar{V}/\omega$	$\bar{\sigma}\,\Delta P/\omega^2$	(Ref 28, page 172)
W_1	$(\overline{\sigma V}/\omega)(\omega)(0.0765)\{A_1\}$	
V_S	h_1	(Ref 6, table IIC)
V_1	$\{M_1\}\{V_S\}$	
ρ_1	h_1	(Ref 6, table IIA)
W_2	$\{V_1\}\{\rho_1\}\{A_1\}$	

M = Mach number

ν = Prandtl-Meyer angle - rad.

h = altitude - feet

P = pressure - lb /ft^2

T = temperature - ^{o}R

ρ = density - lb/ft^3

μ = viscosity - lb sec/ft^2

W_1 = weight flow through filter - lb/sec

W_2 = weight flow intercepted by inlet - lb/sec

A_1 = filter area = 0.1946 ft^2

A_2 = inlet area = 1.640 ft^2

$\overline{V}$ = average velocity through filter - ft/sec

Θ_1 = cone half angle at inlet = $19^\circ 30'$ = 0.34034 rad.

Θ_2 = cone half angle at outlet = 0.01625 rad.

V_S = velocity of sound - ft/sec

4. Stability

Theoretically, the optimum inlet configuration is one in which there is reduction in flow area (contraction) to slow the flow to Mach 1, a throat in which a normal shock occurs, and then an expansion (de Laval nozzle). In actual practice, the contraction must be less than theoretical to provide sufficient pressure ratio for starting the flow through the inlet. The leading edge causes oblique shocks; therefore, the change to subsonic flow is through a series of oblique shocks. The location of these shocks will remain fixed only under very steady conditions of pressure, etc. To assure flow stability, the inlet is designed to allow the shocks to move without spilling the flow out around the inlet. This is achieved by providing a contraction and then a constant area section. The shocks can move back and forth within the constant area section without causing flow instability. An empirical rule of thumb is that a minimum of two diameters of constant area section, as provided in the present design, will provide flow stability.

5. Particle Flow

If the shock is swallowed in the inlet, the particle concentration in the air entering the inlet is the same as the concentration in the ambient air. If there is spillage around the inlet (detached shock), there is a possibility that some of the particles in the spilled air will not follow the air and will enter the inlet. This occurs even more in supersonic than subsonic flow because the particles, being incompressible, do not lose their velocity across the shock. The heavier particles, of course, have more inertia and tend to enter the inlet even if the gas they were originally in is deflected around the inlet. Figure 7 shows the flow geometry at the inlet.

Calculation of the particle trajectories is very complex and is a function of altitude, Mach number, shock location (which can be approximated, knowing the flow through the payload), and particle density and size. (The basic equations for calculating particle trajectories can be found in references 24 and 25.)

These calculations have been done for a similar case in reference 25. Figure 11 of reference 25 has been redrawn (with dashed-line extrapolations) as figure 8; it shows N_I, fraction of particles impacted (entering the inlet), versus a particle size parameter, N_D.

$$N_D = \left(\frac{\rho V}{18\mu D}\right)^{1/2} d$$

ρ, d, and V are the particle density, diameter, and velocity, respectively. μ is the gas viscosity in back of the shock. D is the channel height in figure 6; an equivalent height is used in the present case as shown in the following calculations.

$$\begin{aligned} a &= \text{flow intake efficiency} \\ &= \text{ratio of air taken into air intercepted} \\ &= \frac{\frac{\pi}{4} D_o^2}{\frac{\pi}{4} D_i^2} = \frac{D_o^2}{D_i^2} \end{aligned}$$

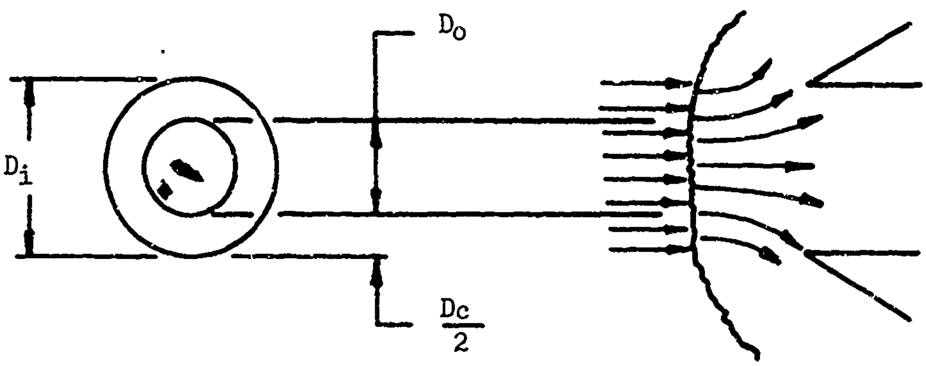

Figure 7. INLET FLOW GEOMETRY

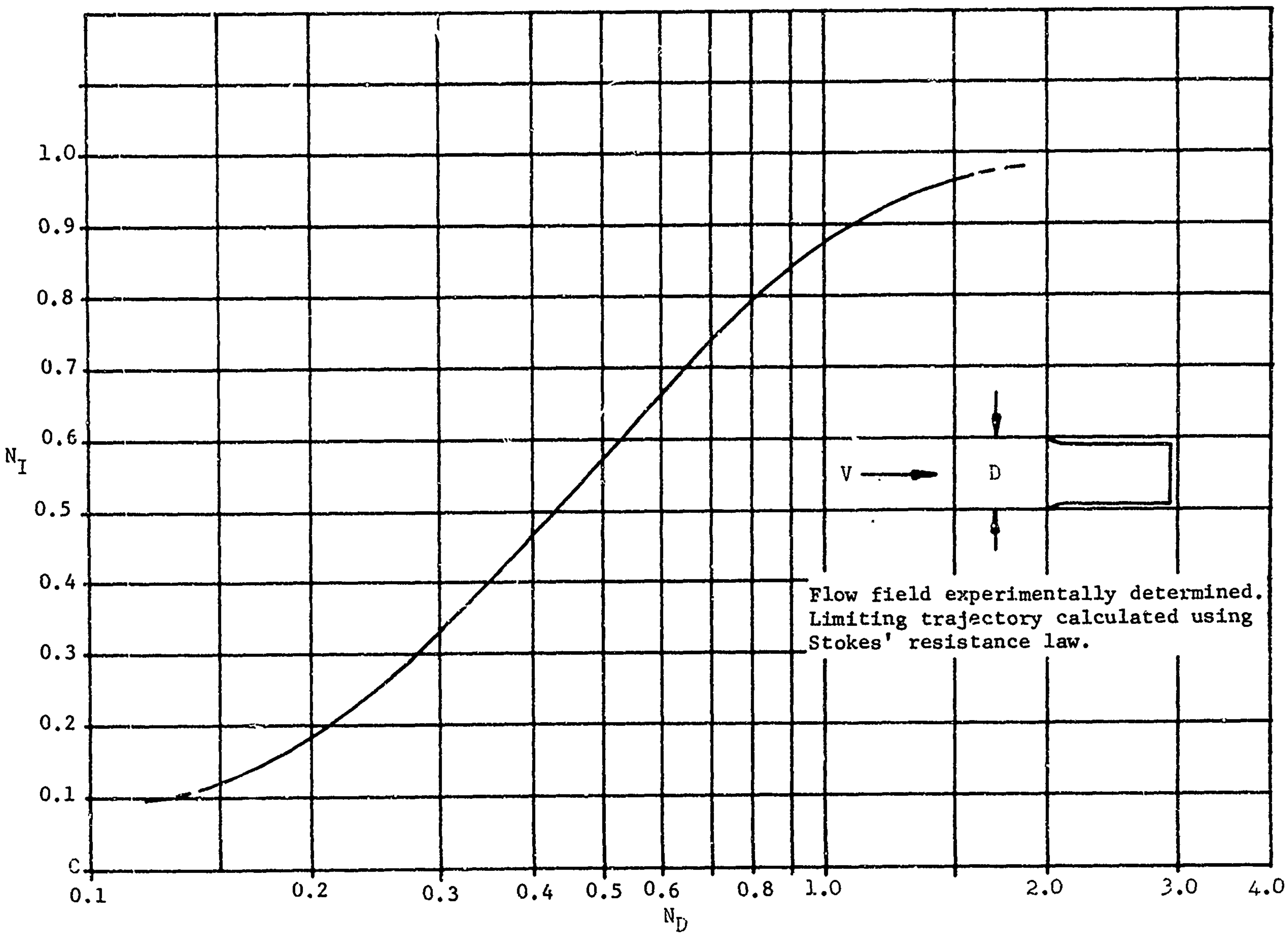

Figure 8. IMPACTION IN A RECESSED COLLECTOR

D_o = diameter of core of air taken in

D_i = inlet diameter = 0.498 ft

D_c = equivalent channel 1 height

$$D_o = (\sqrt{a})(D_i)$$

$$D_c = D_i - D_o = D_i - \sqrt{aD_i} = D_i(1 - \sqrt{a})$$

$$N_D \sim \frac{1}{\sqrt{D_c}} = \frac{1}{\sqrt{D_i(1 - a)}}$$

$$\frac{N_D}{N_D'} = \frac{1}{\sqrt{1 - \sqrt{a}}}$$

N_D' = particle size parameter when a = o (100% spillage).

Fraction of total particles intercepted that are taken in from spilled air = $N_I'(1 - a)$.

Fraction of total particles intercepted that are taken in from air taken in = a.

Fraction of total particles intercepted that are taken in = $N_I'(1 - a) + a$.

Table II shows these flow parameters for the two bounding trajectories.

Figure 8 corresponds to 100 percent spillage. First, plot N_I versus the particle parameters (ρ and D) for various flow conditions with 100 percent spillage (a = o)(figure 9). Second, plot N_I versus a (figure 10). The procedure is to find N_I for a = o from figure 9, and then find N_I for actual a from figure 10. a is found from flow calibration data.

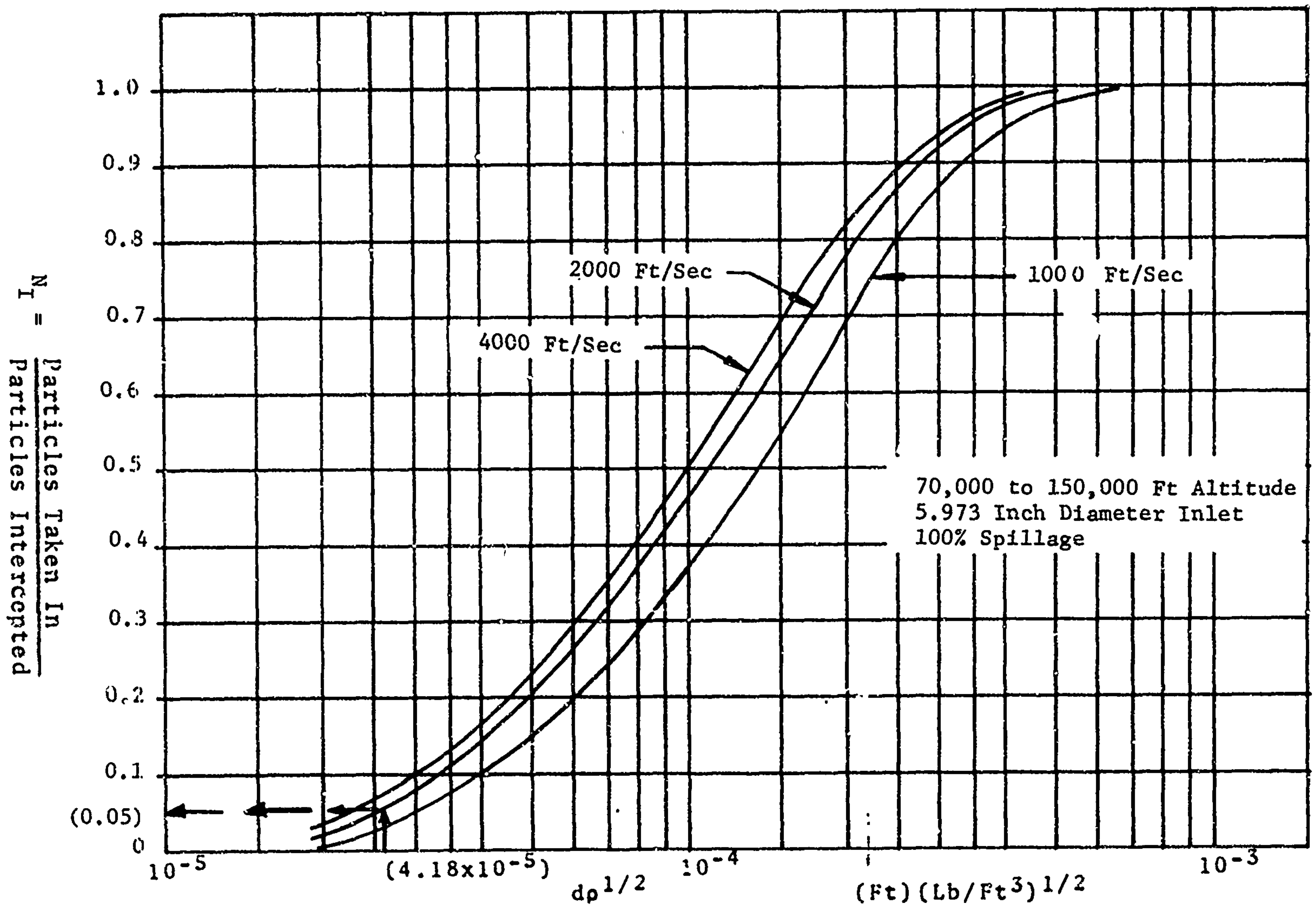

Figure 9
PARTICLE COLLECTION EFFICIENCY
vs. PARTICLE SIZE

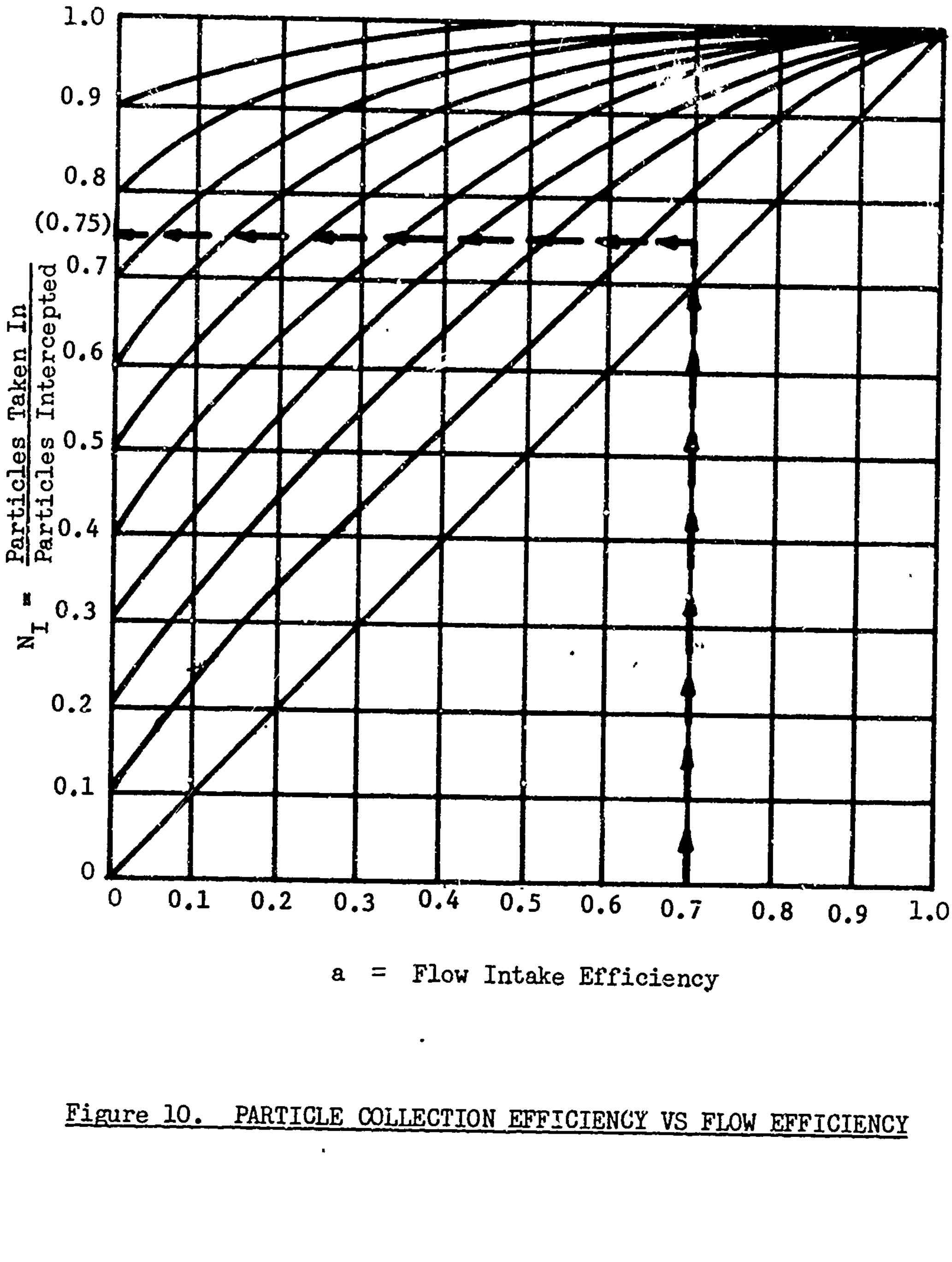

Figure 10. PARTICLE COLLECTION EFFICIENCY VS FLOW EFFICIENCY

TABLE II

FLOW PARAMETERS

Alt $\left(\frac{V_s}{T_1}\right)$ Ft $\left(\frac{Ft/Sec}{°R}\right)$	V_1 Ft/Sec	M_1	$\frac{T_2}{T_1}$	T_2 °R	μ $\frac{Lb\text{-}Sec}{Ft^2}$ x10^6	$\sqrt{\frac{V_1}{18\mu gD}}$	$d\sqrt{\rho}=3\times10^{-5}$ N_D	N_I	$d\sqrt{\rho}=10^{-4}$ N_D	N_I	$d\sqrt{\rho}=3\times10^{-4}$ N_D	N_I
70,000	1,000	1.03	1.020	397	0.310	3,400	0.102	0.05	0.340	0.39	1.02	0.88
$\left(\frac{968}{390}\right)$	2,000	2.07	1.745	680	0.460	3,950	0.109	0.07	0.395	0.46	1.09	0.91
	3,000	3.10	2.799	1,092	0.640	4,100	0.123	0.09	0.410	0.48	1.23	0.93
	4,000	4.13	4.253	1,659	0.832	4,150	0.125	0.09	0.415	0.49	1.25	0.94
150,000	1,000	0.912	1.000	500	0.358	3,170	0.095	0.05	0.317	0.35	0.95	0.86
$\left(\frac{1096}{500}\right)$	2,000	1.82	1.547	603	0.422	4,120	0.124	0.09	0.412	0.48	1.24	0.93
	3,000	2.74	2.386	1,194	0.656	4,050	0.122	0.09	0.405	0.47	1.22	0.93
	4,000	3.65	3.525	1,375	0.738	4,410	0.132	0.10	0.441	0.51	1.32	0.94

$$\sqrt{\frac{1}{18gD}} = \sqrt{\frac{1}{(18)(32.2)(0.498)}} = \frac{1}{16.7}$$

Subscript 1 = Ahead of shock
Subscript 2 = In back of shock

TABLE II (cont'd)

N_D	N_I	a	$\sqrt{a}$	$1-\sqrt{a}$	$\sqrt{1-\sqrt{a}}$	N_D	N_I'	$N_I'(1-a)$	$N_I'(1-a)+a$
0.135	0.1	0.2	0.447	0.553	0.744	0.181	0.16	0.13	0.33
		0.4	0.632	0.368	0.606	0.223	0.22	0.13	0.53
		0.6	0.775	0.225	0.474	0.285	0.31	0.12	0.72
		0.8	0.894	0.106	0.326	0.413	0.48	0.10	0.90
0.210	0.2	0.2				0.282	0.30	0.24	0.44
		0.4				0.347	0.40	0.24	0.64
		0.6				0.443	0.52	0.21	0.81
		0.8				0.643	0.70	0.14	0.94
0.278	0.3	0.2				0.374	0.43	0.34	0.54
		0.4				0.459	0.53	0.32	0.72
		0.6				0.587	0.65	0.26	0.86
		0.8				0.852	0.82	0.16	0.96
0.347	0.4	0.2				0.466	0.54	0.43	0.63
		0.4				0.573	0.65	0.39	0.79
		0.6				0.732	0.76	0.30	0.90
		0.8				1.06	0.90	0.18	0.98
0.427	0.5	0.2				0.574	0.65	0.52	0.72
		0.4				0.705	0.75	0.45	0.85
		0.6				0.902	0.85	0.34	0.94
		0.8				1.31	0.94	0.19	0.98
0.524	0.6	0.2	Same	Same	Same	0.705	0.75	0.60	0.80
		0.4				0.865	0.83	0.50	0.90
		0.6				1.11	0.91	0.36	0.96
		0.8				1.61	0.97	0.19	0.99
0.640	0.7	0.2				0.860	0.83	0.66	0.86
		0.4				1.06	0.90	0.54	0.94
		0.6				1.35	0.95	0.38	0.98
		0.8				1.96	0.98	0.20	1.00
0.800	0.8	0.2				1.075	0.90	0.72	0.92
		0.4				1.32	0.94	0.56	0.96
		0.6				1.69	0.97	0.39	0.99
		0.8				2.45	1.00	0.20	1.00
1.07	0.9	0.2				1.44	0.95	0.76	0.96
		0.4				1.77	0.98	0.59	0.99
		0.6				2.26	0.99	0.40	1.00
		0.8				3.28	1.00	0.20	1.00

For example, determine collection efficiency of 1-micron diameter strontium particles intercepted at 70,000 feet and Mach 2.18.

$$d = 1 \text{ micron} = 3.281 \times 10^{-6} \text{ feet}$$

$$\rho = 162.2 \text{ lb/ft}^3$$

$$d\rho^{\frac{1}{2}} = 4.18 \times 10^{-5} \text{ (ft)}\left(\text{lb/ft}^3\right)^{\frac{1}{2}}$$

Speed of sound at 70,000 feet = 968 ft/sec

Velocity = (2.18)(968) = 2,110 ft/sec

Enter figure 9 at $d\rho^{\frac{1}{2}} = 4.18 \times 10^{-5}$

Move up until 2,110 ft/sec curve intersected (by interpolation between 2,000 and 4,000 ft/sec). Move to left and read $N_I = 0.05$. From figure 17 on page 59 at Mach 2.18 and 70,000 feet, flow intake efficiency = 0.70. Enter figure 10 on bottom at flow intake efficiency = 0.70. Move up intil $N_I = 0.05$ curve intersected (interpolate between $N_I = 0.0$ and 0.1). Move left and read particle collection efficiency = 0.75.

This means that at 70,000 feet and Mach 2.18, 0.70 of the air intercepted (and the particles in that air) is sampled. Of the 0.30 of the air intercepted that spills, an additional 0.05 of the total 1-micron strontium particles intercepted are not spilled and are also sampled.

SECTION IV

FUNCTIONAL ANALYSIS

All mechanical and electrical systems that are required to operate during the flight were analyzed to determine that they would function properly.

a. Nose Tip Actuation

Figure 11 shows the geometry of one-half of the ejectable nose tip. The most severe condition for ejection encountered on a nominal trajectory are:

Altitude = 69,900 ft

Dynamic pressure (q) = 744 lb/ft^2

which occurs 20 seconds after launch and at Mach 3.36 (Ref 10).

$$D = C_D A q = \text{(drag coefficient)(area)(dynamic pressure)}$$

$$C_{D_1} = .84 \text{ (reference 9, page 121)}$$

$$A_a = \frac{\pi}{4}\left(\frac{6.80}{12}\right)^2 \frac{1}{2} = 0.1260 \text{ ft}^2$$

$$D_1 = (0.84)(0.1260)(744) = 78.8 \text{ lb}$$

$$C_{D_1} = 2.00 \text{ maximum for blunt bodies (reference 20, pages 213-224).}$$

$$A_b = 0.1482 \text{ ft}^2 \text{ (reference Dwg 63D15411)}$$

$$D_2 = (2.00)(0.1482)(744) = 220.5 \text{ lb}$$

Assume pivoting around corner

$$F = \frac{(78.8)(3.400) + (220.5)(2.156)}{1.750}$$

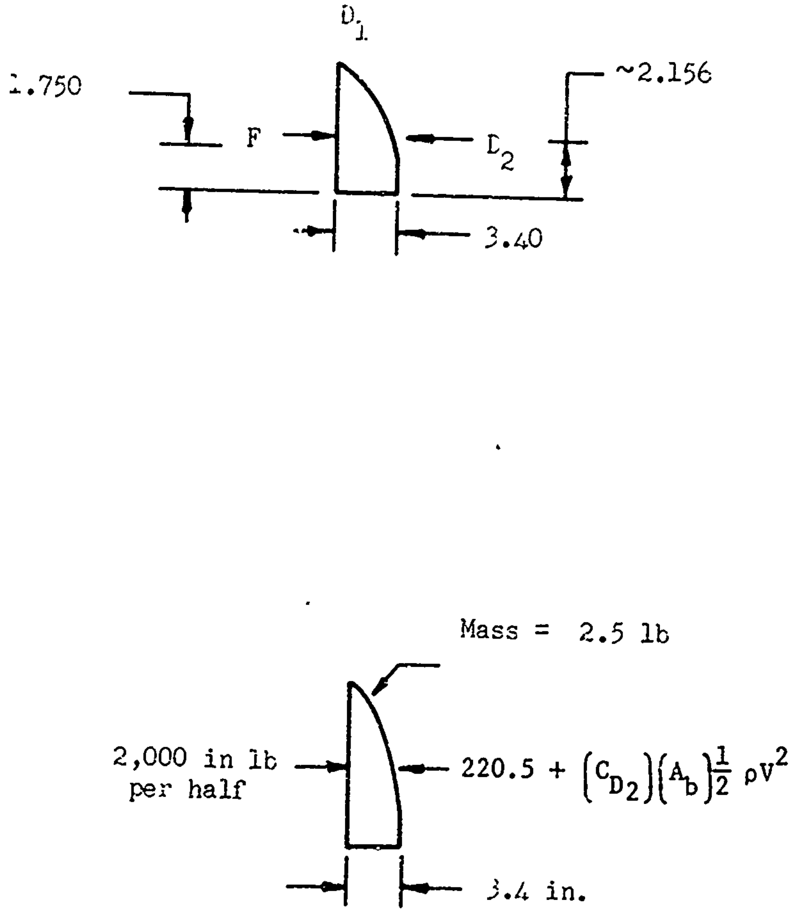

Figure 11. NOSE TIP GEOMETRY

$$= \frac{267.9 + 475.4}{1.750} = \frac{743.3}{1.750}$$

$$= 424.7 \text{ lb}$$

F available = 800 ± 200 lb minimum (specified)

= 2,680 lb (measured)

$$\text{Minimum S.F.} = \frac{600}{424.7} = \underline{1.41}$$

For a 3.40-inch stroke:

Energy required = (424.7)(3.400) = 1,444 in-lb

Energy available = 4,000 in-lb/min (specified)

= 4,020 in-lb (measured)

$$\text{S.F.} = \frac{4,000}{1,444} = \underline{2.77}$$

Assume no pressure equalization:

ΔP across tip = 14.7 psi = 2,118 psf

$$F = (\Delta P)(A) = (2,118)(0.1260) = 267 \text{ lb}$$

$$\text{S.F.} = \frac{600}{267} = \underline{2.25}$$

Velocity of halves: Temporarily neglect $C_{D_2} A_b \frac{\rho V^2}{2}$. Assume radial motion of half and 3.4 inches of travel until clear of payload.

Energy absorbed = (220.5)(3.4) = 750 in-lb

Net energy = 2,000 - 750 = 1,250 in-lb

= 104.2 ft-lb

$$= \frac{1}{2} \frac{W}{g} V^2$$

$$104.2 = \frac{1}{2} \left(\frac{2.5}{32.2}\right) V^2$$

$$V^2 = 2{,}682$$

$$V = 51.5 \text{ ft/sec}$$

Check $C_{D_2} A_b \dfrac{\rho V^2}{2}$

$$\rho = 1.40 \times 10^{-4} \text{ lb sec}^2/\text{ft}^4 \text{ (reference 6)}$$

$$C_{D_2} A_b \frac{\rho V^2}{2} = \frac{(2.00)(0.1482)\left(1.40 \times 10^{-4}\right)(2{,}682)}{2}$$

$= 0.0556$ lb, which is negligible

b. Band Release

63C15461 Band

$$\text{Energy} = \int_0^l \frac{M^2}{2EI}\,dx \qquad \text{(Ref 19, page 190)}$$

$$M = \frac{EI}{r} \qquad \text{(Ref 3, page 122)}$$

$$\text{Energy} = \int_0^{2\pi r} \left(\frac{EI}{r}\right)^2 \frac{1}{2EI}\,dx$$

$$= \frac{EI}{2r^2}\, x \Big]_0^{2\pi r}$$

$$= \frac{\pi EI}{r}$$

$$I = \frac{bh^3}{12}$$

$$= \frac{(21.21)(0.030)^3}{12}$$

$$= 4.98 \times 10^{-6}$$

$$\text{Energy} = \frac{(\pi)\left(30 \times 10^6\right)\left(4.98 \times 10^{-6}\right)}{8.43}$$

$$= 55.7 \text{ in-lb} = 4.64 \text{ ft-lb}$$

$$\text{Weight} = (2\pi)(8.43)(2.2\text{[illegible]})(0.030)(0.286)$$

$$= 1.005 \text{ lb}$$

$$4.64 = \frac{1}{2}\left(\frac{1.005}{32.2}\right) V^2$$

$$V^2 = 297.6$$

$$V = 17.24 \text{ ft/sec}$$

This is the average velocity of the band as it leaves the payload.

c. Door Closure

63C15429 spiral torsion spring provides closing force.

$$\frac{M}{N} = \frac{\pi E b h^3}{6L} \qquad \text{(Ref 2, page 48)}$$

$$= \frac{(\pi)\left(30 \times 10^6\right)(1.5)(0.0720)^3}{(6)(130)}$$

$$= 67.8 \text{ in-lb/rev}$$

$$N = \frac{M}{67.8}$$

$$= \frac{60}{67.8} = 0.884 \text{ rev}$$

$$M = (67.8)(N)$$

$$= (67.8)(0.884 + 2.50)$$

$$= 76.9 \text{ in-lb}$$

d. Aft Plate Closure

The 63C15486 helical compression spring provides closing and sealing force.

Length in closed position = 5.45 in.

$$\text{Sealing force } F = \frac{\Delta\ell \; G \; d^4}{8 \; D^3 \; N} \qquad \text{(Ref 2, page 20)}$$

$$\Delta\ell = 30.45 - 5.45 = 25.00$$

$$G = 11.5 \times 10^6 \qquad \text{(Ref 2, page 11)}$$

$$F = \frac{(25.00)\left(11.5 \times 10^6\right)(0.343)^4}{(8)(16.032)^3(3.5)}$$

$$= 34.5 \text{ lb}$$

$$\text{Spring weight } W = (N)(\pi D)\left(\frac{\pi}{4} d^2\right) \rho$$

$$= (4.5)(\pi)(16.032)\left(\frac{\pi}{4}\right)(0.343)^2(0.286)$$

$$= 6.0 \text{ lb}$$

$$\text{Net force} = F - W = 34.5 - 6.0 = 28.5$$

$$\Delta\ell = 30.45 - 2.62 = 27.83$$

$$F = \frac{(27.83)\left(11.5 \times 10^6\right)(0.343)^4}{(8)(16.032)^3(3.5)} = 38.4 \text{ lb}$$

e. Electrical System

Battery voltage = 4.5V (Eagle-Picher 485R Silver-Zinc "A" cells)

Bolt squibs = 0.18 ± 0.03 ohm (Holex Series 250 Explosive Bolts)

Nose tip squibs = 1.00 ± 0.30 ohm each, 4 in. parallel (Hercules Mark 1, Mod 0 Detonators)

$$\text{Bolt squib current} = \frac{4.5}{0.18 \pm 0.03} = 25.0^{+5.0}_{-3.6} \text{ amps.}$$

All fire current = 2.0 amps (Ref 21)

$$\text{Min SF} = \frac{21.4}{2.0} = 10.7$$

Nominal firing time = 0.17 millisecond (Ref 21)

Fuse firing time (Littelfuse 314003) = 23 millisecond (Ref 22, page 31)

$$\text{Nose tip squib current} = \frac{4.5}{1.00 \pm 0.30}$$

$$= 4.50 \begin{smallmatrix} +1.93 \\ -2.04 \end{smallmatrix} \text{ amps per squib}$$

All fire current = 1.50 amps (Ref 31)

$$\text{Min SF} = \frac{3.46}{1.50} = 2.31$$

Nominal firing time < 0.0007 seconds (Ref 31)

Current for 4 squibs = (4)(4.50) = 18.0 amps

Fuse firing time = 0.4 seconds (Ref 22, page 31)

= 400 milliseconds

Maximum battery current = 25.0 amps

Discharge time = 1.7 minutes (Ref 23, page 1A-2)

Battery nominal capacity = 35 amp-min. (ibid)

Maximum allowable current = 40 amps for 1 min. discharge time (ibid)

SECTION V

STRESS ANALYSIS

Stresses were analyzed in all parts subjected to any significant loading from aerodynamic forces; rocket acceleration, shock, and vibration; aircraft acceleration; parachute opening shock; snatch acceleration and shock; and unequalized pressures. The worst conditions of combined loading were considered. The minimum yield safety factor and ultimate safety factor were over 1.50.

a. Aerodynamic Loads

Lift:

Flight maximum

$L = 435$ lb (Ref 16)

$CP =$ Sta 20.95 (ibid)

Drag:

Flight maximum (same conditions as lift)

C_D (ogive) $= 0.106$ (Ref 8, page 236)

C_D (sphere) $= 0.88$ (Ref 9, page 121)
(based on sphere radian)

$$C_D \text{ (sphere)} = 0.88 \left(\frac{2.59}{8.675}\right)^2$$

$= 0.078$, based on ogive radius

$$\text{Total } C_D = 0.106 + 0.078 = 0.184$$

$q = 7{,}000$ lb/ft^2 (Ref 16)

$$D = (C_D)(q)(A)$$

$$= (0.184)(7{,}000)(1.642)$$

$$= 2{,}114 \text{ lb}$$

b. Design Loads

Table III summarizes the design loads. The maximum forward and side loads are caused by motor burn; the maximum aft load, by parachute deployment.

TABLE III

DESIGN LOADS

ITEM	FORWARD		AFT		SIDE	
	g	lb	g	lb	g	lb
Acceleration	100	13,500	40	5,400	5	675
Shock	100	13,500	50	6,750	16	2,160
Vibration	16	2,160	16	2,160	9	1,215
Maximum	100	13,500	50	6,750	16	2,160
Max. Combined	100	13,500	16	2,160	9	1,215

c. Outer Shell

(1) Bending & Axial

$$S_1 = \frac{M}{Z}$$

M = 1,215 (Sta 18.00) max. combined

M = 2,160 (Sta 18.00) max. individual

$$S_z = \frac{F}{A} = \frac{13,500}{A}$$ max. combined or individual

$$S = S_1 + S_2 \qquad USF = \frac{30,000}{S}$$ @ 500°F (Ref 11)

Table IV summarizes these quantities.

TABLE IV

BENDING & AXIAL STRESSES

STA	RAD	T	Z	M	S_1
28.00	8.20	0.080	16.85	12,150 21,600	722 (combined) 1,285 (individual)
35.26	8.58	0.125	28.71	20,970 37,300	731 (combined) 1,300 (individual)

STA	A	S_2	S_{max}	USF
28.00	4.123	3,270 3,270	3,992 3,270	7.52 (combined) 9.18 (individual)
35.26	6.74	2,000 2,000	2,731 2,000	11.0 (combined) 15.0 (individual)

(NOTE: YS not definable. Proportional limit ≈ 50 - 60% of US at room temperature (reference 13, page 9).

(2) Buckling due to Column Loading

Assume 120 lb of payload weight on shell.

$$F = W\ddot{X} = (120)(100) = 12{,}000$$

$$\text{Buckling } S = K\sigma\left(E_{f\alpha} + E_{f\beta}\right)\frac{t}{r} \quad \text{(reference 13, page 137)}$$

$$S = \frac{F}{A} = \frac{F}{2\pi rt}$$

$$\text{Buckling } F = 2\pi K\sigma\left(E_{f\alpha} + E_{f\beta}\right)t^2$$

$$E_{f\alpha} = E_{f\beta} = 2 \times 10^6 \ @\ 500^\circ F \quad \text{(reference 11)}$$

$$K\sigma = 0.12 \quad \text{(reference 13, page 138)}$$

$$\text{Buckling } F = (2)(\pi)(0.12)\left(4 \times 10^6\right)(0.080)^2$$

$$SF = \frac{\underline{19{,}300}}{12{,}000} = \underline{1.61}$$ (NOTE: Stiffening effect of inlet and stiffeners are not considered.)

d. Outer Stiffener

(1) Bending & Axial Loads

Compression = 100 g x 120 lb = 12,000 lb

M = 1,215 (Station 18.00) max. combined

M = 2,160 (Station 18.00) max. individual

$$S_1 \quad \frac{M}{Z}$$

$$S_2 = \frac{F}{A} - \frac{12{,}000}{A} \text{ maximum combined or individual}$$

$$S = S_1 + S_2$$

Station 32.210 - 8.40 rad.

Consider eight 0.063 x 1.000 stiffeners as a uniform cylinder.

$$Z = r^2 t = (2\ rt)\left(\frac{r}{2}\right) = (A)\left(\frac{r}{2}\right)$$

$$= [(8)(0.063)(1.000)]\ \frac{8.400}{2}$$

$$= (0.504)(4.200)$$

$$= 2.116$$

M = 17,265 (combined)

M = 30,700 (individual)

$$S_1 = \frac{17{,}265}{2.116} = 8{,}159 \text{ (combined)} \quad S_1 = \frac{30{,}700}{2.116} = 14{,}508 \text{ (indiv.)}$$

$$S_2 = \frac{12{,}000}{0.504} = 23{,}809$$

S = 31,968 (combined)

S = 38,318 (max. individual)

$$\text{YSF} = \frac{64{,}000}{38{,}318} = \underline{1.67} \qquad \text{(Ref 14, 3.2, 7.0)}$$

$$\text{USF} = \frac{76{,}000}{38{,}318} = \underline{1.98} \qquad \text{(ibid)}$$

(NOTE: Stiffener assumed to take all load at this station. Strength of outer shell neglected.)

(2) Buckling

$$P_{cr} = \frac{4\pi^2 EI}{L^2} \qquad \text{(Ref 3, page 294)}$$

$$E = 10.5 \times 10^6 \qquad \text{(Ref 14, 3.2, 7.0b)}$$

$$I = \frac{(1)(0.063)^3}{12} = 2.08 \times 10^{-5}$$

$$P_{cr} = \frac{(4)\left(\pi^2\right)\left(10.5 \times 10^6\right)\left(2.08 \times 10^{-5}\right)}{(2.00)^2}$$

$$= 2{,}155$$

$$S_{cr} = \frac{P_{cr}}{A} = \frac{2{,}155}{(1)(0.063} = 34{,}206$$

$$\text{SF} = \frac{76{,}300}{34{,}206} = \underline{2.23}$$

(NOTE: Stiffener assumed to take all load at this station. Strength of outer shell neglected.)

e. Attachment of

63J15471, Outer Shell
63D15481, Aft Ring
LL54G82P8, Long-Lok Screw

Screw transmit bending moment; forward load transmitted directly. Figure 12 shows the dimensions of the screws.

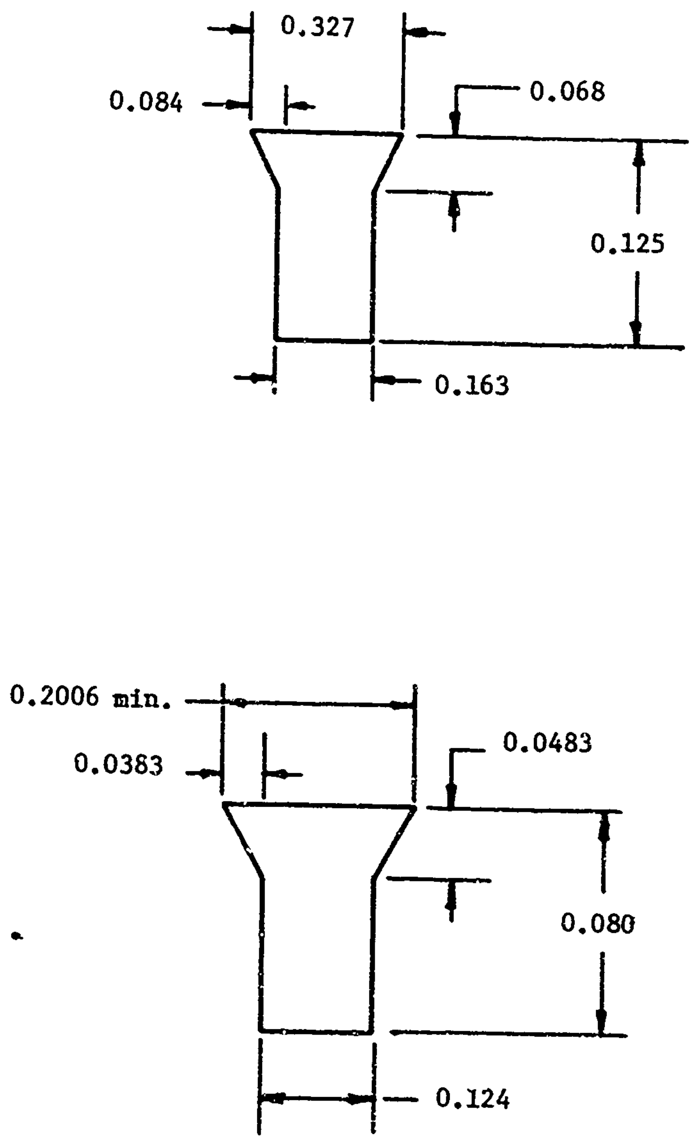

Figure 12. SCREW DIMENSIONS

Station 35.622, 17.080 dia. (63D15481)

$$M = 2{,}160 \text{ (Sta 18.00) maximum}$$

$$= 2{,}160\ (35.622 - 18.00)$$

$$= 38{,}100$$

$$F = \frac{38{,}100}{\frac{\pi}{4}(17.080)^2} = 166.0 \text{ lb/in. of circ.}$$

$$S = \frac{\pi(17{,}080)}{30} = 1.789 \text{ in. of circ./screw}$$

$$F = (166.0)(1.789) = 297.2 \text{ lb/screw}$$

#8-32 at minor dia. $A = \frac{\pi}{4}(0.125)^2 = 0.01227$

$$S_s = \frac{297.2}{0.01227} = 24{,}220$$

$$USF = \frac{40{,}000}{24{,}220} = \underline{1.65} \qquad \text{(Ref 14, 2.2, 3.0)}$$

(Figure 12 shows the dimensions of the screws.)

Bearing on outer shell:

$$A = (0.163)(0.125) + (0.084)(0.068)$$

$$= 0.02037 + 0.00571$$

$$= 0.02608$$

$$S = \frac{297.2}{0.02608} = 11{,}420$$

$$USF = \frac{30{,}000}{11{,}420} = 2.62 \text{ @ } 500^{\circ}F \qquad \text{(Ref 11)}$$

f. Attachment of

63J15471, Outer Shell
63C15472, Stiffener (8)
MS20427M4-4, Rivet (96)
MS20427M4-5 (56)
5481C and 5441, Fiber-Resin Adhesive

Rivets and adhesive transmit bending moment; forward load transmitted directly.

Station 32.650, 8.46 rad.

$$M = 2{,}160 \text{ (Sta 18.00) maximum}$$

$$= 2{,}160\ (32.650 - 18.00)$$

$$= 31{,}630$$

$$\frac{I}{A} = 2(8.46)^2 + 4[(0.707)(8.46)]^2$$

$$= 143.1 + 143.1 = 286.2$$

$$F = \frac{MR}{I/A} = \frac{(31{,}630)(8.46)}{286.2} = 936 \text{ lb/stiffener}$$

Consider only three rivets at Station 32.65 $= (3)\frac{\pi}{4}(0.124)^2$ $(49{,}000) = 1{,}185$ lb min before driving (reference MS20427).

Adhesive $= (0.4)(1.00)(2{,}000) = 800$ lb (reference 15)

Total $= 1{,}185 + 800 = 1{,}985$

$$USF = \frac{1{,}985}{936} = \underline{2.12}$$

Rivets bearing on shell:

$$\frac{\pi/4(0.124)^2(49{,}000)}{2.12} = 186 \text{ lb/rivet}$$

$$A = (0.124)(0.08) + (0.0383)(0.04483)$$
$$= 0.00993 + 0.00185$$
$$= 0.01178$$

$$S = \frac{186}{0.01178} = 15{,}800$$

$$USF = \frac{30{,}000}{15{,}800} = \underline{1.90} \text{ @ } 500^{\circ}F$$ (reference 11)

g. Attachment of

63J15471, Outer Shell
63C15472, Stiffener (8)
MS20427M2-4, Rivet (112)
5410 and 5441, Fiber-Resin Adhesive

Bearing on shell plus compression of shell at stiffeners.

$$A = (0.045 + 0.050)(1)(8)$$
$$= (0.095)(1)(8)$$
$$= 0.760$$
$$F = 12{,}000$$

$$S = \frac{12{,}000}{0.760} = 15{,}800$$

$$USF = \frac{30{,}000}{15{,}800} = \underline{1.90} \text{ @ } 500^{\circ}F$$ (reference 11)

h. Attachment of

63J15471, Outer Shell (1)
63J15420, Inlet Assembly (2)
LL54D62P12, Long-Lok Screw (16 ea) (3)
LL14G02P5, Long-Lok Screw (16 ea) (4)

(Figure 13 shows the attachment geometry.)

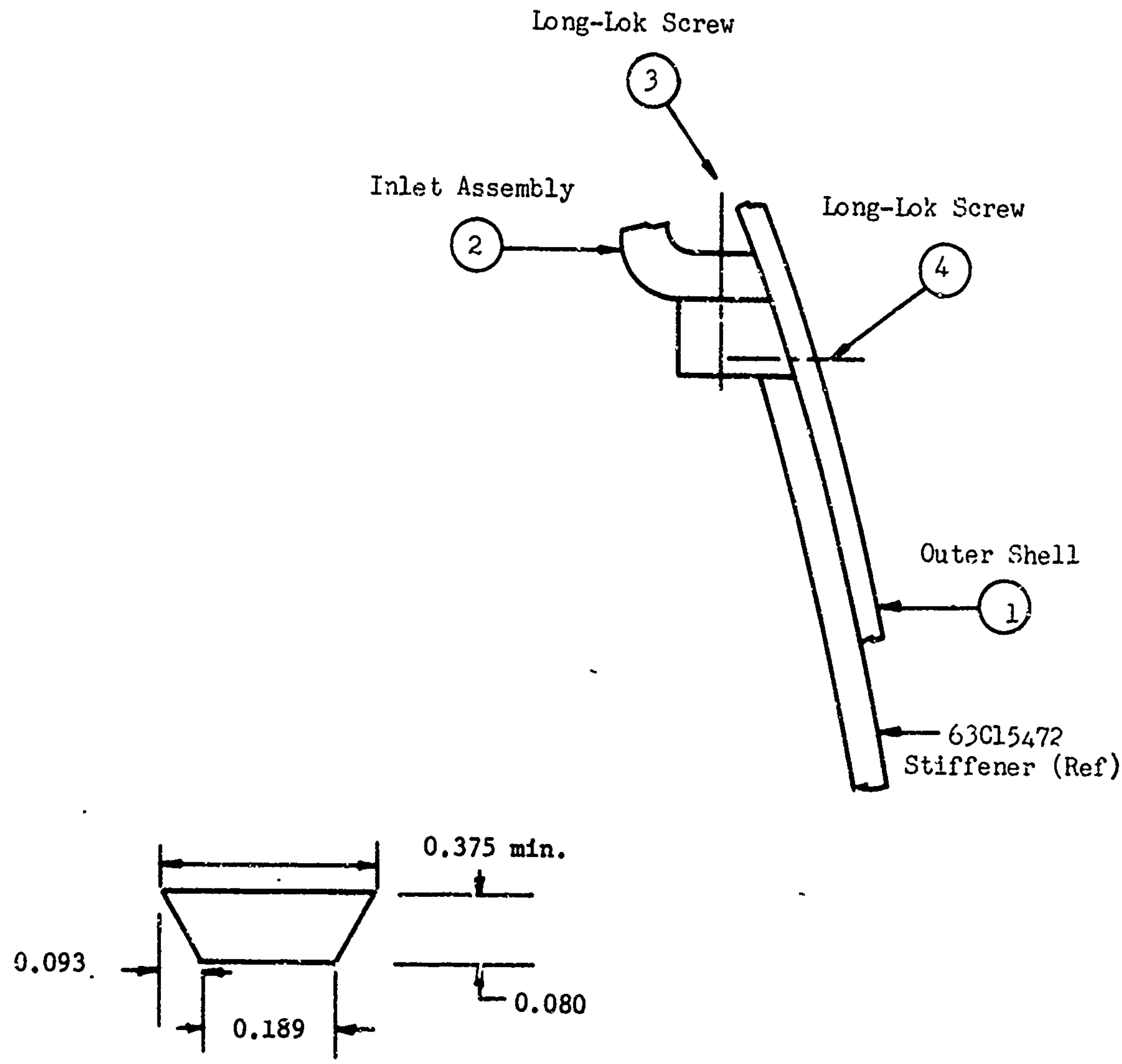

Figure 13. ATTACHMENT GEOMETRY

$$A = 0.189\ (0.080) + (0.093)(0.080)$$

$$A = 0.01513 + 0.00744$$

$$A = 0.02257$$

$$F = W\ddot{X} = 120\ (50) = 6{,}000$$

$$S = \frac{F}{NA} = \frac{6{,}000}{16(0.02257)} = 16{,}614$$

$$USF = \frac{30{,}000}{16{,}614} = \underline{1.80} \text{ @ } 500^{\circ}F \quad \text{(reference 11)}$$

Tension load in inlet assembly mounting screws.

$$F = W\ddot{X} = 120\ (50) = 6{,}000$$

Ultimate load per screw = 790 lb

$$USF = \frac{790(16)}{6{,}000} = \underline{2.1}$$

i. Band

$$S_t = \frac{Ey}{\rho} \quad \text{(reference 3, page 121)}$$

$$\rho = 8.37 \quad \text{(Ref 63J15471, Outer Shell)}$$

$$S_t = \frac{(30 \times 10^6)}{(8.37)} \quad \text{(Ref 2, page 10)}$$

$$= 71{,}600 \text{ psi}$$

$$YSF = \frac{120{,}000}{71{,}600} = \underline{1.67} \quad \text{(ibid)}$$

$$USF = \frac{160{,}000}{71{,}600} = \underline{2.23} \quad \text{(ibid)}$$

j. Spiral Torsion Spring

$$S_t = \frac{6M}{bh^2} \quad \text{(Ref 2, page 48)}$$

$$= \frac{(6)(80)}{(1.47)(0.0720)^2}$$

$$= 63{,}000 \text{ psi}$$

$$YSF = \frac{125{,}000}{63{,}000} = \underline{1.98} \qquad \text{(Ref 2, page 10)}$$

$$USF = \frac{160{,}000}{63{,}000} = \underline{2.54} \qquad \text{(ibid)}$$

k. Helical Compression Spring

$$S_s = \frac{8PD}{\pi d^3} \qquad \text{(Ref 1, page 11-02)}$$

$$= \frac{(8)(50)(16.032)}{\pi(0.343)^3}$$

$$= 50{,}500 \text{ psi}$$

$$C = \frac{D}{d} = \frac{16.032}{0.343} = 46.7 \qquad \text{(Ref 1, page 11-03)}$$

$$K = \frac{4C-1}{4C-4} + \frac{0.615}{C} \qquad \text{(ibid)}$$

$$= \frac{(4)(46.7)-1}{(4)(46.7)-4} + \frac{0.615}{46.7}$$

$$= 1.02 + .01$$

$$= 1.03$$

$$S_s = KS_s \qquad \text{(ibid)}$$

$$= (1.03)(50{,}500)$$

$$= 52{,}000$$

$$YSF = \frac{80{,}000}{52{,}000} = \underline{1.54} \qquad \text{(Ref 2, page 11)}$$

$$USF = \frac{115{,}000}{52{,}000} = \underline{2.21} \qquad \text{(ibid)}$$

l. Channel

g Loads: Bending due to plate, spring, channel.

$$F = W\ddot{X} = (20)(100) = 2{,}000$$

Consider as built-in beam with center load.

$$M = \frac{Fl}{8} \qquad \text{(Ref 17, page 108)}$$

$$= \frac{(2{,}000)(15{,}380)}{8}$$

$$= 3{,}845$$

$$Z = 1.38 \qquad \text{(Ref 18, page 222)}$$

$$S = \frac{M}{Z}$$

$$= \frac{3{,}845}{1.38}$$

$$= 2{,}786$$

$$YSF = \frac{33{,}000}{2{,}786} = \underline{11.8} \qquad \text{(Ref 14, 3.2, 6.0)}$$

$$USF = \frac{36{,}000}{2{,}786} = \underline{12.9} \qquad \text{(ibid)}$$

m. Attachment of

63D15482, Channel

63D15481, Aft Ring

MS16997-24, Sch Cap Screw 6-32 (2)

MS16998-31, Sch Cap Screw 10-32 (4)

g Loads: Shear due to plate, spring, and channel.

$$F = W\ddot{X} = (20)(100) = 2{,}000$$

$$A = (2)\left(\frac{\pi}{4}\right)(0.0997)^2 + (4)\left(\frac{\pi}{4}\right)(0.1517)^2$$

$$= 0.01562 + 0.0723$$

$$= 0.08792$$

$$S = \frac{F}{A} = \frac{2,000}{0.08792} = 22,747$$

Min UTS = 160,000 (Ref MS16997 and MS16998)

Assume min UYS $\geq$ 1/2 min UTS = 80,000

$$USF = \frac{80,000}{22,747} = \underline{3.51}$$

n. Inner Screen

Side g Load: Consider as a cantilever beam 9.66 in. long.

Measured weight = 6 lb

$$\text{Cylinder area} = [\pi(12.54) + 0.13][9.41 + 0.25]$$

$$= (39.40 + 0.13)(0.66)$$

$$= 382 \text{ in}^2$$

$$\text{Plate area} = \frac{\pi}{4}(12.54)^2$$

$$= 123.5 \text{ in}^2$$

$$CG \approx \frac{(382)(4.83) + (123.5)(9.66)}{382 + 123.5}$$

$$= \frac{1,845 + 1,192}{505.5}$$

$$= \frac{3,037}{505.5} = 6.01 \text{ in.}$$

For 16 g:

$$M = (16)(6)(6.01)$$

$$= 577 \text{ in lb}$$

$$Z \approx \frac{AD}{4}$$

$$\text{Number of wires} = \pi D8$$

$$= (\pi)(12.54)(8) = 315$$

$$\text{Wire area} = \frac{\pi}{4}(0.017)^2 = 0.000227$$

$$A = (315)(0.000227) = 0.0716$$

$$\dot{Z} = \frac{(0.0716)(12.54)}{4} = 0.2044$$

$$S = \frac{M}{Z} = \frac{577}{0.2044} = 2{,}822$$

$$YSF = \frac{30{,}000}{2{,}822} = \underline{10.6} \qquad \text{(Ref 14, 2.2, 3.0)}$$

$$USF = \frac{75{,}000}{2{,}822} = \underline{26.6} \qquad \text{(ibid)}$$

Axial g Load:

$$F = W\ddot{x} = (6)(100)$$

$$= 600 \text{ lb}$$

$$A = 0.0716$$

$$S = \frac{F}{A} = \frac{600}{0.0716} = 8{,}379$$

$$YSF = \frac{30{,}000}{8{,}379} = \underline{3.58} \qquad \text{(Ref 14, 2.2, 3.0)}$$

$$USF = \frac{75{,}000}{8{,}379} = \underline{8.9} \qquad \text{(ibid)}$$

o. Outer Screen

Side and axial g loads. Dimensions are approximately the same as for 63D15442 inner screen. Therefore, safety factors will be approximately the same. Min SF was 3.58 on YS and 8.9 on US.

p. Pressure Equalization in Flight

From ground to launch elevation (35,000 ft), the pressure is equalized through various joints in the payload because of time available during aircraft flight. After rocket launch, assume no equalization and zero pressure outside.

At 35,000 feet

$$P = 499.3 \text{ psf} \qquad \text{(Ref 6, page 79)}$$

$$= 3.47 \text{ psi}$$

(1) Outer Shell (63J15471)

$$S = \frac{Pr}{t} \qquad \text{(Ref 17, page 268)}$$

$$= \frac{(3.47)(8.20}{0.08}$$

$$= 355$$

$$USF = \frac{30{,}000}{355} \text{ @ } 500^{\circ}F \qquad \text{(Ref 11)}$$

$$= \underline{84.5}$$

SECTION VI

WEIGHT & CG ANALYSIS

Requirements were a weight of 135 ± 5 pounds, with the center of gravity forward of missile station 18.0. Initially, approximate weights and CG's were calculated and appeared to meet the requirements. As parts were fabricated, actual weights and CG's were determined. The inlet weight was reduced slightly to ensure compliance with the requirements. Final determination of weight and CG of the payload was by actual measurement and not by calculation. The weight was found to be 136.4 pounds, with the center of gravity at mission station 18.0 on the first complete payload. Since all payloads are essentially identical, all will meet the requirements.

SECTION VII

ENVIRONMENTAL TESTING

Environmental testing consisted of longitudinal and lateral load testing of a payload. An axial compression test was performed by Aerolab Development Company; the rest of the tests were performed by the AFSWC.

a. Axial Compression

Prior to final testing at the AFSWC, a preliminary test was performed at Aerolab Development Company to ensure the payload would pass the forward acceleration and shock tests. These were the two most severe load tests. The major effect on the payload of forward acceleration is to cause the heavy inlet assembly (102 pounds) to come loose from the outer shell and move aft. Axial compression between the forward end of the inlet and the aft end of the outer shell would produce the same effect. Therefore, an axial compression test was performed using a hydraulic press to apply the load. Load was measured by a pressure gage on the press. Deflection of the payload was measured with dial indicators. The load was applied and removed in about 500-pound increments and readings taken at each increment. The equivalent g loading was calculated by dividing the load by the inlet assembly weight (102 pounds). Results are plotted in figure 14. The straight-line relationship between load and deflection up to the maximum load of 145 g indicates no permanent deformation (yielding) of the payload. Deviations of individual points from the line are within the limits of error in readings of load and deflection. The relationship between load and deflection upon removal of the load indicates hysteresis in the system. Settling of parts of the load-applying and deflection-measuring setups, rather than the payload itself, probably accounted for much of the hysteresis.

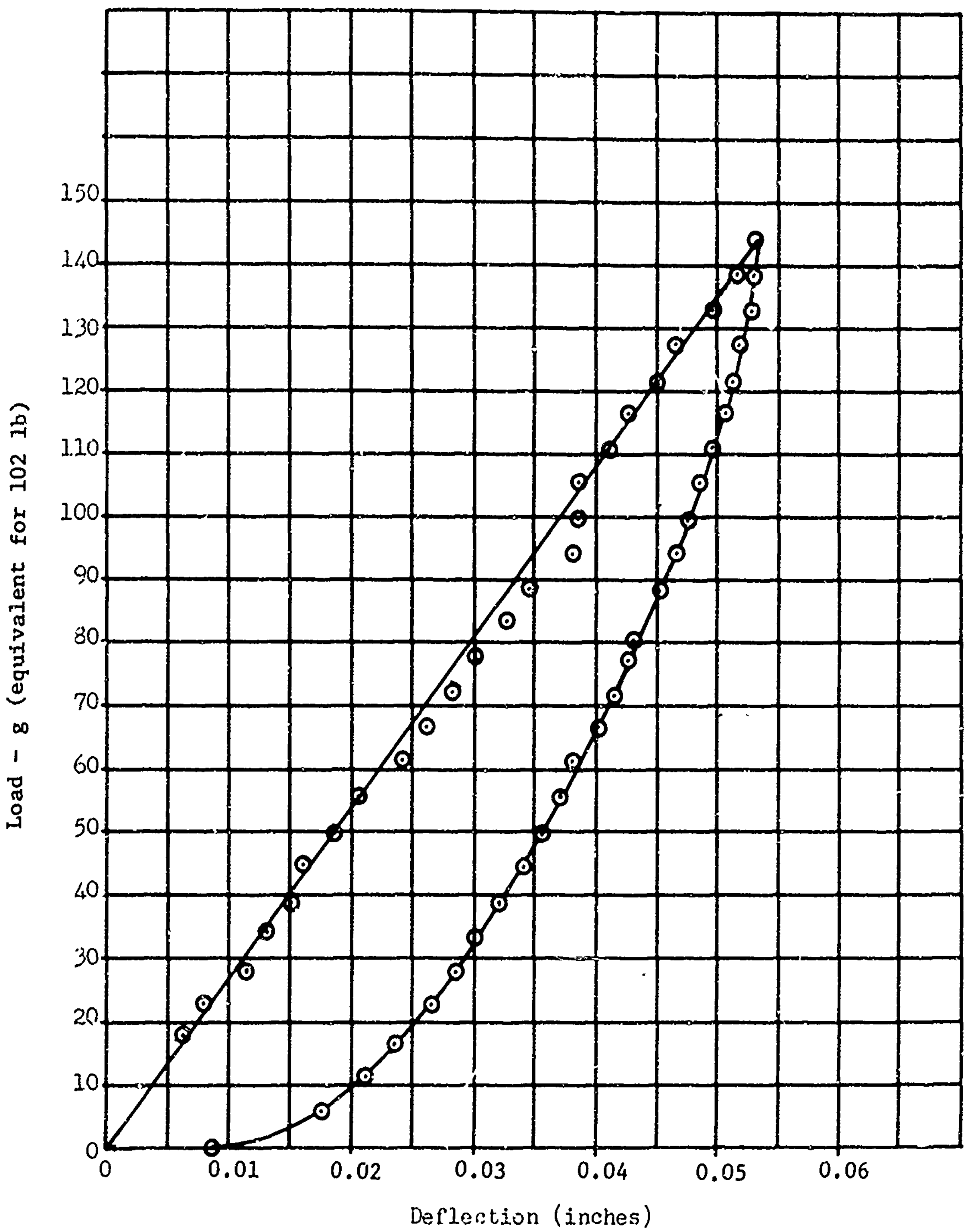

Figure 14

LOAL VS DEFLECTION AXIAL COMPRESSION BETWEEN INLET & AFT RING

b. Shock

The payload was subjected to a forward square-wave shock of 52 g for 11 milliseconds and showed no signs of damage.

c. Vibration

The payload was subjected to longitudinal and then lateral sinusoidal vibration by an electromechanical shake. Longitudinal vibration was from 20 to 2,000, and then back to 20 cycles per second. From 20 to 100 cps, double amplitude was 0.01 inch. From 100 to 2,000 cps, the intensity was 9 g. As the frequency returned to 20 cps, the nose tip assembly appeared to be loose. Examination indicated one of the retainers holding the tip to the inlet had slipped off the edge of the slot in the inlet. The retainer was found to have been improperly installed. It was then properly installed, and no further difficulty was encountered in either vibration or acceleration tests. The payload was then vibrated at 16 g between 220 and 260 cps for 1 minute.

Similar tests were then performed laterally. Double amplitude between 20 and 100 cps was 0.01 inch, the intensity between 100 and 2,000 cps was 7 g, and intensity between 220 and 260 cps was 9 g. Vibration intensity versus frequency is shown in figure 15 and 16 for longitudinal and lateral vibration, respectively. Both test conditions and DM14 missile flight data (reference 32) are shown.

No evidence of damage or loosening of parts was found at the completion of the vibration tests.

d. Acceleration

The payload was subjected to lateral and then forward acceleration in a centrifuge. Maximum speed during lateral acceleration was 70.7 rpm. The payload center of gravity was 74.2 inches from the

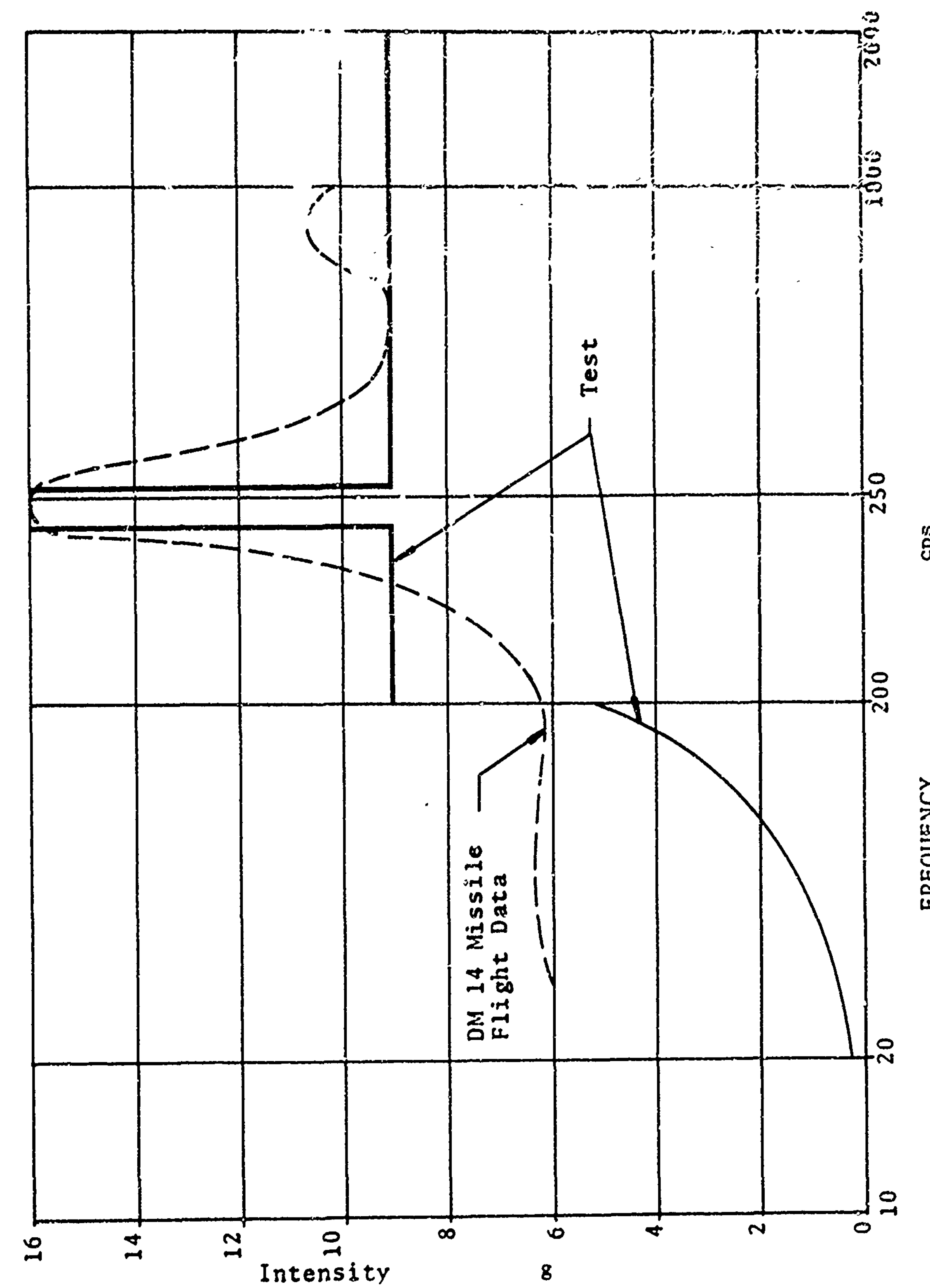

Figure 15

LONGITUDINAL VIBRATION vs. FREQUENCY

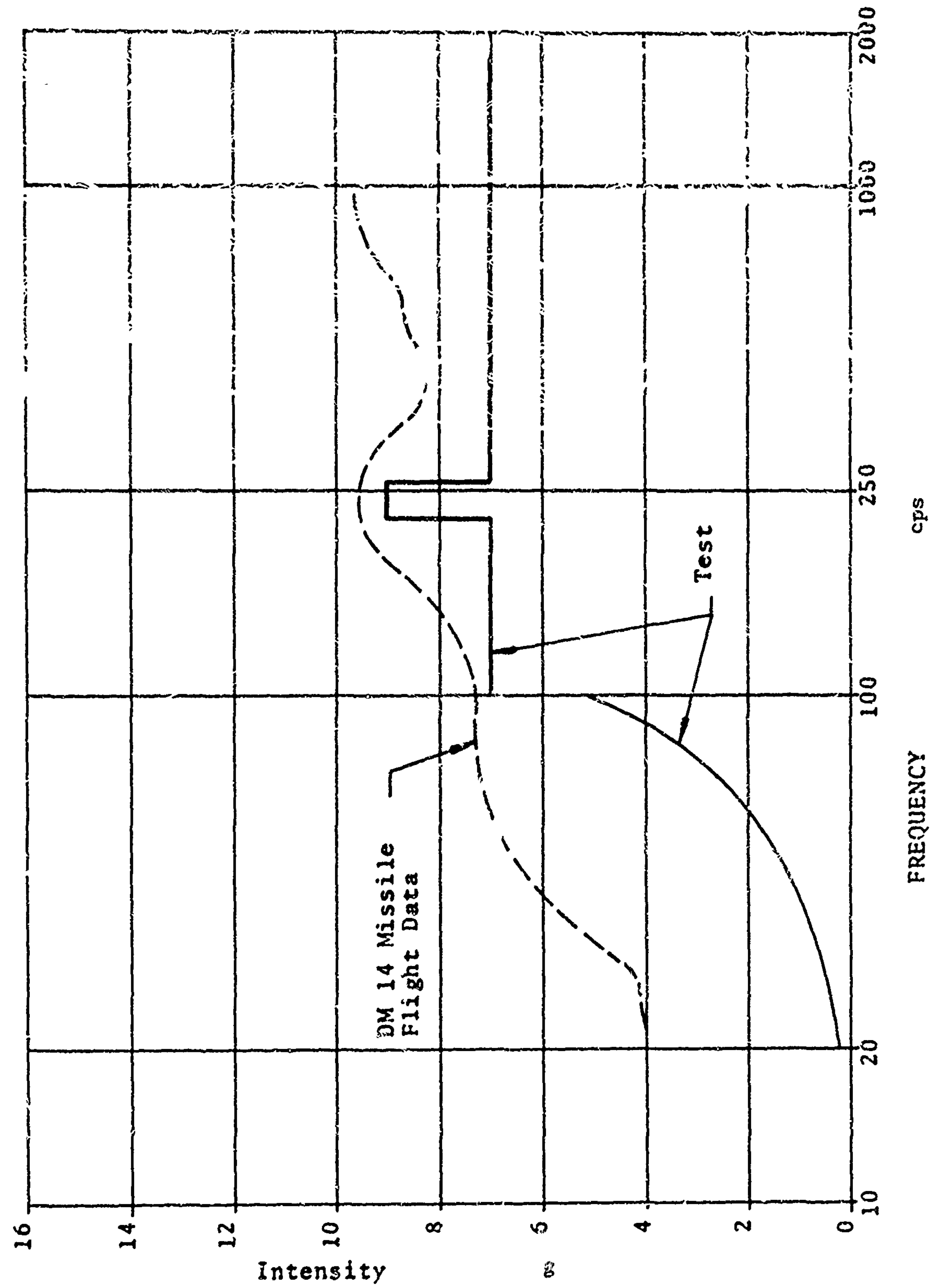

Figure 16

LATERAL VIBRATION vs. FREQUENCY

center of rotation with the outer edges at 65.5 and 82.9 inches. Calculated acceleration at the CG was 10.5 g, with 9.3 and 11.8 g at the edges.

Maximum speed during forward acceleration was 236.3 rpm. The CG was 51.0 inches from the center of rotation, with the forward end at 33.8 inches and the aft end at 65.5 inches. Calculated acceleration at the CG was 81.0 g, with 53.6 g at the forward end and 111.5 g at the aft end.

No evidence of damage or permanent deformation was found at the completion of the acceleration tests.

SECTION VIII

FLOW TESTING

Flow testing consisted of measuring the air flow rate intercepted by the payload inlet and the air flow rate intake efficiency under simulated flight conditions. The tests were performed in the 16-foot supersonic tunnel (16S) at Arnold Engineering Development Center (AEDC) by ARO, Inc.

a. Test Procedure

A payload for ALARR was instrumented to measure pressure and temperature forward and aft of the basket. The wind tunnel was instrumented to measure flow conditions in the tunnel. The payload was placed in the tunnel, and flow conditions at several altitudes and Mach numbers were simulated. Flow rate through the inlet was determined by using the basket itself as a meter. Flow rate through the basket, which is equal to flow rate through the inlet, can be determined from the basket area and the upstream and downstream pressures and temperatures from the data in reference 28 - specifically, figure 45, which plots a modified pressure drop versus a modified flow rate. Flow rate intercepted by the payload inlet was determined from tunnel flow rate and inlet area. The ratio of flow through the inlet to flow intercepted by the inlet was defined as flow intake efficiency and is the parameter of interest at each altitude and Mach number. Details of the test procedures are in reference 34.

b. Test Results

Test results were reported in references 33, 34, 35, and 36. References 33 and 35 are preliminary, unchecked data from the two test series, and reference 34 is the final report based on the data contained in reference 33. Flow rates were incorrect in reference 33, but were corrected in reference 36. Since no final report is forthcoming on the second test series, the preliminary unchecked data in reference 35 are assumed valid for the second test series.

Test results from the first series showed:

(1) Both the cylinder-plate and cylinder-cone basket configurations are structurally acceptable.

(2) The cylinder-plate configuration has a higher flow intake efficiency.

(3) Maximum flow intake efficiency is achieved at maximum exit area (existing configuration) down to approximately half of the maximum exit area, with the tendency to buzz about the same over this range.

The cylinder-plate basket configuration with maximum exit area was therefore selected for the final configuration. Table V compares flow intake efficiency of the final configuration with the cylinder-cone configuration for the only two cylinder-cone configuration points with maximum exit area. At smaller exit areas the efficiencies are about the same.

During the second test series, several internal modifications were made by ARO, Inc. They were adding inlet rake, adding another basket screen, increasing the splitter plate area, and some combinations of the above. They all reduced flow intake efficiency; therefore, they are not considered either desirable modifications or conditions yielding valid data points. Valid data points from both test series are shown in figure 17, along with theoretical flow intake efficiency curves.

Because of the limited number of points, no meaningful curves could be drawn through the points. For six points (noted in figure), data at angles of attack up to 5° were obtained. No change in flow efficiency occurred between 0° and 5° angle of attack.

TABLE V

FLOW INTAKE EFFICIENCY COMPARISON

Test 1

BASKET CONFIGURATION	CYLINDER-CONE	CLYINDER-PLATE
Altitude (ft)	70,200	70,000
Mach Number	2.199	2.195
Basket Flow (lb/sec)	0.89	1.34
Intake Flow (lb/sec)	1.91	1.91
Flow Intake Efficiency	0.47	0.70

Test 2

BASKET CONFIGURATION	CYLINDER-CONE	CYLINDER-PLATE
Altitude (ft)	70,800	70,600
Mach Number	1.700	1.700
Basket Flow (lb/sec)	0.62	0.84
Intake Flow (lb/sec)	1.36	1.35
Flow Intake Efficiency	0.46	0.62

Maximum Exit Area

Zero Angle of Attack

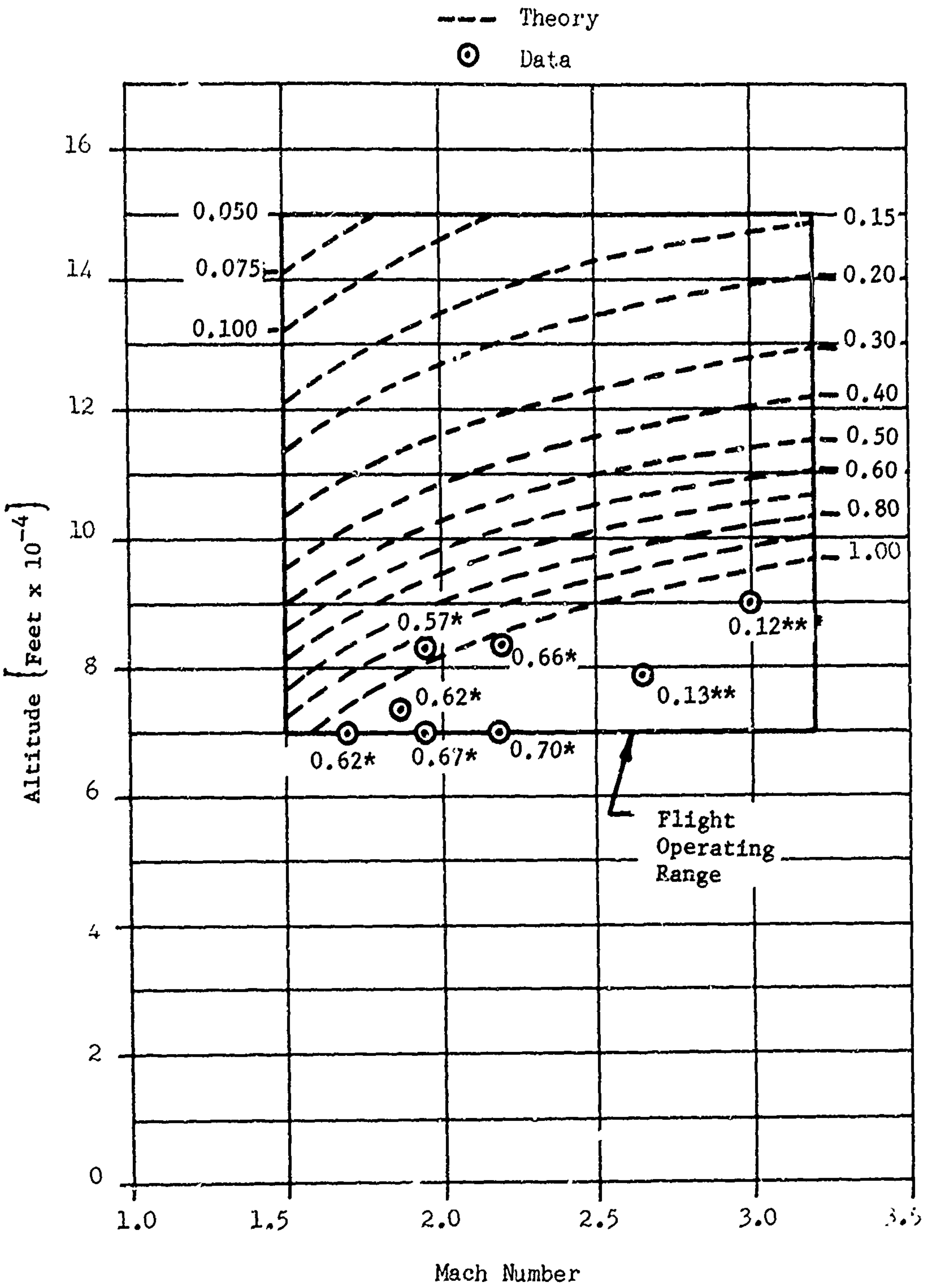

Figure 17. FLOW INTAKE EFFICIENCY

(At Various Altitudes & Mach Numbers - Exit Area = 6.30 ft^2)

SECTION IX

FUNCTIONAL TESTING

1. Nose Tip

The nose tip explosive actuator was mounted in a load testing machine and initiated. The actuator produced an average thrust of 2,680 pounds over a 1.50-inch stroke, or an energy output of 4,020 inch-pounds. Minimum requirements were 800 pounds thrust and 4,000 inch-pounds energy output. The complete nose tip was ejected successfully during flow testing at AEDC. The complete nose tip was again ejected successfully during the flight test on the ALARR vehicle.

2. Band

The band was ejected successfully during flow testing at AEDC and again during the flight test.

3. Door

The door in the inlet was tested repeatedly for proper closing by releasing it manually. The door closed properly during the flight test.

4. Aft Plate

The aft plate was tested repeatedly for proper closing by releasing it manually. The payload was too badly damaged in the flight test to determine how the aft plate operated.

5. Electrical Circuit

The batteries, heater, and fuses were mounted on the channel that is part of the aft assembly. This unit was cooled with dry ice, and the temperature was held at -65°F or less. Quick acting fuses with firing characteristics similar to the squibs used in the payload were used to simulate the squibs. A manual switch was used in place of the timer in the payload. First, the nose tip and band circuits were actuated by means of the switch. Both fuses (simulating the squibs) blew. Next, these two circuits were then shorted to simulate shorting of the circuits during actual firing, although the possibility of shorting is very remote. The two protective fuses in the electrical circuit blew. Finally, the door and aft plate circuits were actuated, and both fuses (simulating the squibs) blew.

These tests showed that (1) under the worst conditions of temperature and battery drain, all squibs could still be fired, and (2) the fuses protected the batteries from excessive drain even in case of a dead short.

SECTION X

CONCLUSIONS AND RECOMMENDATIONS

Mechanically, electrically, and structurally, the payload for ALARR meets all of the specifications. However, flow intake efficiency is not as great as predicted theoretically. Recommendations for improvement of the payload are:

a. Flow test the unit at additional simulated altitudes and Mach numbers so flow intake efficiency can be calibrated over a greater part of the flight operating range.

b. Perform flow tests to determine pressure losses in each part of the unit (inlet, diffuser, basket, and outlet).

c. Investigate methods of reducing pressure losses and increasing flow intake efficiency.

d. Perform flow tests on unit, incorporating improvements to increase flow intake efficiency.

SECTION XI

FUTURE PLANS

Several new inlet configurations are being designed by the Flight Dynamics Laboratory, Wright-Patterson AFB, Ohio. Wind tunnel tests of an Aerolab payload with these various inlets are planned for April 1966; however, these changes will not be incorporated in the four existing payloads. Flight test of the existing Aerolab payloads are scheduled to begin in September 1966.

REFERENCES

1. Kent's Mechanical Engineers' Handbook, Design and Production, John Wiley & Sons, 1950.

2. Handbook of Mechanical Spring Design, Associated Spring Corporation, 1963.

3. Timoshenko, S., Elements of Strength of Materials, D. Van Nostrand Company, Inc., 1951.

4. Pre-test Information in Accordance with Section 7.1 of Vol 3 of Test Facilities Handbook for Payload for ALARR, AFSWC Contract AF 29(601)-6248.

5. Ames Research Staff, Equations, Tables, and Charts for Compressible Flow, NACA Report No. 1135, 1953.

6. Minzner, Champion, and Pond, The ARDC Model Atmosphere, 1959, AFCRC TR-59-267, 1959.

7. Exhibit "A" to Purchase Request No. SWT-412, AFSWC, 29 Nov 1963.

8. Morrison, Design Data for Aeronautics and Astronautics, John Wiley & Sons, Inc., 1962.

9. Lubliner, Oliver, Morgan, Low-to-High-Speed Drag Compilations for Rocket Test Sled Configurations, NAVORD Report 5635, 1957.

10. Trajectory #4 for PR SWT-412, 30-Degree Launch, AFSWC, 1963.

11. MIL-R-9299A, Resin, Phenolic, Low-Pressure Laminating, Type II, Class I.

12. ALARR Environmental Design and Test Load Conditions, Cook Electric Company, 1964.

13. Plastics for Flight Vehicles, Part 1, Reinforces Plastics, MIL-HDBK-17, 1959.

14. Strength of Metal Aircraft Elements, MIL-HDBK-5, 1961.

15. Fiber-Resin Corporation, Burbank, California.

16. ALARR Payload Attachment Fastener Design Stress Analysis, Cook Electric Company, 10 Dec 1963.

17. Roark, Formulas for Stress & Strains, Third Edition, McGraw-Hill Book Co., Inc., 1954.

18. Alcoa Structural Handbook, Aluminum Company of America, 1960.

19. Hartog, Den, Mechanical Vibrations, Third Edition, McGraw-Hill Book Co., Inc., 1947.

20. Morrison & Ingle, Design Data for Aeronautics & Astronautics, John Wiley & Sons, Inc., 1962.

21. Holex, Inc., Technical Data Sheet, Holex Series 2500 Explosive Bolts, Rev C, 1 Feb 1963.

22. Littelfuse, Inc., Catalog #15.

23. Special Batteries, The Eagle-Picher Company.

24. Triutt, R. W., Hypersonic Aerodynamics, The Ronald Press Company, 1959.

25. Ranz, W. E., Principles of Inertial Impaction, The Pennsylvania State University, 1956.

26. Eshbach, O. W. Handbook of Engineering Fundamentals, John Wiley & Sons, Inc., 1961.

27. Wu, Chapkis, and Mager, Approximate Analysis of Thrust Vector Control by Fluid Injection, ARS Journal, Dec 1961.

28. Dearth, L. R. and Van der Akker, J. A., Study of the Filtration and Permeability Characteristics of IPC 1478 Filter Paper, AD-235-318,

29. Society of Automotive Engineers, Aeronautical Information Report #24, 1 Feb 1952.

30. Price List & Specifications No. 455, Diamond Metal Sales.

31. Product Data - Squib, Mk 1 Mod 0, Hercules Powder Company, 12 Aug 1960.

32. DM-14 Missile Flight Vibration Vs Frequency, Report SM-27125.

33. ALARR Systems Test - Propulsion Wind Tunnel, Supersonic (16S) - Propulsion Wind Tunnel Facility, (AEDC) - Tabulated Data, ARO, Inc., Arnold AF Station, Tenn., May 1964.

34. Perkins, T. M., Investigation of the Internal Flow Characteristics of the ALARR Payload, AEDC TDR 64-197, Sep 1964.

35. ALARR Systems Test #2 - Propulsion Wind Tunnel, Supersonic (16S) - Propulsion Wind Tunnel Facility, AEDC - Inlet-Exhaust Flow Data, ARO, Inc., Arnold AF Station, Tenn., Jan 1965.

36. ALARR System Test in 16S - Corrected Data, Tab 4, ARO, Inc., Arnold AF Station, Tennessee.

SUPPLEMENTARY

INFORMATION

AD-480 062

AIR FORCE SPECIAL WEAPONS CENTER
Air Force Systems Command
Kirtland Air Force Base
New Mexico

29 April 1966

ERRATA

AFSWC-TR-65-6 PAYLOAD FOR ALARR (Unclassified Report)
March 1966

Page 63: Replace page 63 with attached page.

Authority:
Richard G. Grisham
1Lt USAF

C. W. Haig

C. W. HAIG
Chief, Reports and Data Branch
Technical Information Division

1 Atch
Page 63 of AFSWC-TR-65-6

SECTION XI

FUTURE PLANS

Two versions of a replacement sampler for the Aerolab payload have been designed by Professor Hal Larsen, head of the Aeronautical Engineering Department of the Air Force Institute of Technology (AFIT), with the assistance of his students and staff. The most promising version employs a spike, similar to those commonly employed in ramjet applications, and a supersonic diffuser which permits maximum pressure recovery. Theoretical calculations indicate that it is capable of "isokinetic" sampling up to 150,000 feet with the mach number equal to or greater than 1.75. Higher altitudes are, of course, possible at higher mach numbers. This device will require 1/4 basis weight IPC filter paper above about 125,000 feet. The second version consists of a supersonic inlet and a subsonic diffuser, both designed to permit maximum pressure recovery. Theoretical calculations indicate that it is capable of "isokinetic" sampling up to about 125,000 feet with the mach number equal to or greater than 2.0. This will require 1/4 basis weight IPC filter paper above 110,000 feet.

Wind tunnel tests of these payloads are planned to begin in April 1966 at the Arnold Engineering Development Center (AEDC). The models for these tests are currently being built by AFIT, under the supervision of Professor Larsen who will be in charge of the tests.

Assuming satisfactory wind tunnel test results, a contractor will be selected to construct flight test versions of the most promising configuration and Professor Larsen will act as a consultant during this and the ensuing flight tests, pending further approval. Assuming satisfactory flight test results, this device will be phased in as a replacement for the Aerolab payload.